BL1A

Si K-Edge XANES Study of Fe- and/or Ga-Substituted MFI Metallosilicates

H. Aritani[1], S. Koyama[1], K. Otsuki[1], A. Nakahira[2], H. Matsuhashi[3]

[1]*Faculty of Engineering, Saitama Institute of Technology, Fukaya 369-0293, Japan*

[2]*Graduate School of Engineering, Osaka Prefecture Universitty, Sakai*

[3]*Faculty of Education, Hokkaido University of Education, Hakodate 040-8567, Japan*

Zeolites are well known as microporous materials, and have been applied widely to several engineering processes because of peculiar surface activity based on acidity. They are open framework aluminosilicates consisting of SiO_4 and AlO_4, interconnected *via* oxygen atoms. Both Si and Al are present with T_d symmetry in zeolite framework. But distortion is often brought about by application of several thermal processes or reactions. MFI-type zeolite is one of a typical material for application of catalysts with unique activity. In particular, Cu^{2+} ion-exchanged H-MFI shows high deNO_x activity with hydrocarbons. But an important problem due to hydrothermal stability cannot be avoided in the case of modified MFI. On the other hand, metallosilicates are one of the appropriate materials because active cations (trivalent transition metal ions mainly) are incorporated onto zeolite framework. For example, Fe^{3+}-substituted MOR zeolites show high NO-SCR activity with methane.[1] But deactivation proceeds during the reaction, as a major subject. We synthesized Fe- and Ga-MFI with various metal ratios by hydrothermal synthesis. Fe^{3+}- and Ga^{3+}-co-substituted MFI (FeGaMFI) can be obtained. These materials show unique reactivity for NO_x-SCR; FeMFI with high Fe ratio shows high NO-SCR activity but no activity for NO_x-SCR (in coexistence of O_2). In contrast, GaMFI with high Ga ratio shows high activity for NO_x-SCR. In order to clarify the structural stability of zeolite framework over Fe- and/or Ga-substituted MFI metallosilicates, Si K-edge XAFS study is applied to characterize the local symmetry of Si atoms. KTP(011) monochromator gave more emission of soft X-ray source in the region of 1.2 - 2.1 keV,[2] and thus, accurate XANES can be obtained. In recent studies, Si K-edge XANES can give an information about the local symmetry of SiO_4 structure, reported by Tanaka et al.[3] and other workers. In our study, XANES at Si K-edge was applied to characterize the several types of zeolites in order to evaluate the possibility of characterization around Si atom. Fe- and/or Ga-substituted MFI (FeMFI, GaMFI, FeGaMFI) materials were obtained by hydrothermal synthesis, and followed by calcination at 873 K. Molecular ratio of Si/Al_2 is 72 in each materials, and Al^{3+} site is substituted to Fe^{3+} and/or Ga^{3+}. The XANES spectra at Si K-edges were measured in BL1A of UVSOR in a total electron yield mode at ambient temperature by using KTP(011) monochromator.

Fig. 1 shows the XANES spectra of FeMFI (100% of substituted Fe ratio), FeGaMFI (Fe 75%, Ga 25%), and GaMFI (Ga 100%) before/after the reaction. For FeMFI, white line due to SiO_4 tetrahedra in MFI framework can clearly be seen. The intensity of the peak is larger than that of H-MFI (consist of SiO_2-Al_2O_3), indicating highly symmetric T_d sites are formed. In contrast, the intensity in Ga-substituted MFI is slightly smaller than that of H-MFI, as well as that of FeGaMFI. These results suggest that Fe substitution brings about structural change of MFI framework, and Ga co-substitution inhibit the structural change. It is likely that Fe sites in FeMFI are less stable than Ga sites in MFI structure, supporting the results of Fe and Ga K-edge XAFS. After the reaction, the intensity in FeMFI becomes larger. It suggests the structural change due to separation of Fe site by hydration. But Ga site is almost stable for the reaction. It can be expected that the FeGa co-substituted MFI is appropriate for NO-SCR catalyst because of structural stability of active Fe sites with Ga sites. Detailed study is now in progress.

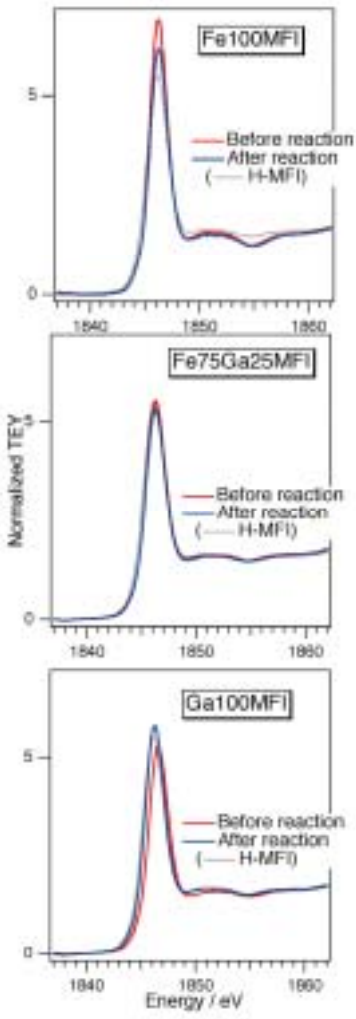

Fig. 1 Si K-edge XANES of FeMFI, FeGaMFI, and GaMFI before/after MOx-SCR with methane at 873 K for 3 h.

[1] H. Aritani *et al.*, Chem. Mater. **14** (2002) 562.
[2] Y. Takata *et al.*, J. Synchrotron Rad. **8** (2001) 351.
[3] T. Tanaka *et al.*, J. Phys. **IV** (Colloq. C2) (1997) 913.

BL1A

Evaluation of Catalytically Active Mo Species on H-MFI for Methane Dehydroaromatization

H. Aritani[1], S. Shinohara[1], S. Koyama[1], K. Otsuki[1], K. Saito[1], T. Kubo[2], A. Nakahira[2]
[1]*Faculty of Engineering, Saitama Institute of Technology, Fukaya 369-0293, Japan*
[2]*Graduate School of Engineering, Osaka Prefecture Universitty, Sakai 599-8531, Japan*

Many workers have focused on this catalyst system as a novel GTL process from natural gas to petroleum products since Wang et al. reported the methane dehydroaromatization over MoO_3/H-MFI catalysts in absence of oxygen. It has been revealed that reduction of Mo^{6+} ions is brought about in contact with methane in the initial step, and then Mo ions react methane to form carbide species, Mo_2C, in the next step. It is thus accepted that active Mo species are consist of reduced ions, Mo^{2+}, with Mo-carbide and/or oxycarbide species on H-MFI. On the other hand, molybdena catalysts supported on silica-alumina-based supports also show the dehydroaromatization activity. The activity for converting methane and its deactivation rate depend on the property of silica-alumina supports. In fact, molybdena supported on amorphous silica-alumina also shows dehydroaromatization activity, while it is lower than that on H-MFI. Relation between the silica-alumina support (with surface acidity) and active Mo species formed in the reaction is thus important to clarify the formation process of highly active Mo. In this study, Mo L_{III}-edge XANES is applied to characterize the Mo species on H-MFI and silica-alumina supports.

All the catalysts were prepared by impregnation of each silica-alumina support with ammonium heptamolybdate solution (7.5wt% loading as MoO_3), and followed by drying and calcination at 773 K for 3 h. Amorphous SiO_2-Al_2O_3 (containing 28.6 wt% Al_2O_3; denoted as SAH-1) and H-MFI (Si/Al_2=40, 90, 1880) supports were employed. Mo L_{III}-edge XANES spectra were measured in BL1A of UVSOR-IMS in total-electron yield mode.

Figure 1 shows the L_{III}-edge XANES spectra of reference samples. It is clear that edge energy values of XANES spectra in MoO_2, α-Mo_2C and Mo metal are different from each other. To clarify the difference, second derivatives of XANES spectra are also shown. The difference of energy value is significantly between Mo_2C (at 2525.3 eV) and Mo metal (at 2524.7 eV). This assignment can be applied to characterize the reduced Mo ions. As a reference, the spectrum of partially oxidized Mo_2C (denoted as Mo_2C (oxd.)), which is calcined at 473 K for 0.5 h, is also shown in Figure 1. The energy of a first minimum peak (at 2525.7 eV) is higher than that of bare Mo_2C but lower than that of MoO_2. Because stable Mo oxy-carbide does not exist commercially, the Mo_2C (oxd.) can be applied as a reference oxy-carbide sample. Figure 2 shows the L_{III}-edge XANES spectra of MoO_3/SAH-1 and MoO_3/H-MFI (Si/Al_2=90, showed maximum activity for benzene production) catalysts before/after the reaction. For

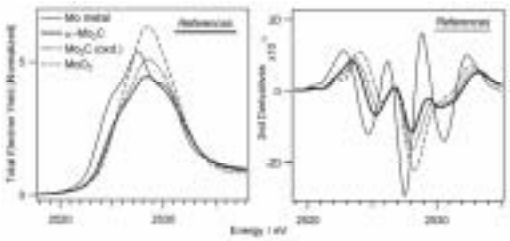

Fig. 1 Mo L_{III}-edge XANES spectra (left) and their second derivatives (right) of reference compounds: MoO_2, Mo_2C, partially oxidized Mo_2C and Mo metal.

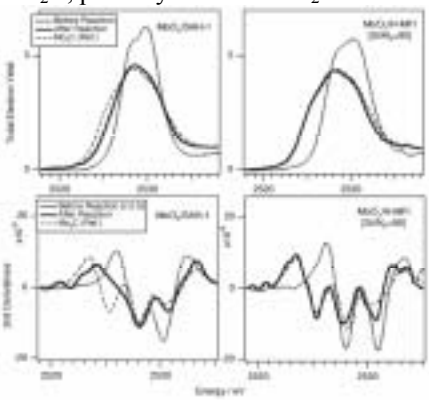

Fig. 2 Mo L_{III}-edge XANES (top) and their second derivatives (bottom) of MoO_2/SAH-1 and MoO_3/H-MFI (Si/Al_2=90) before/after dehydroaromatization of methane at 973 K.

MoO_3/SAH-1, it can be presumed that octahedral Mo^{6+} ions are changed definitely to form reduced species, which has some differences from Mo_2C, by the reaction. Mo^{6+}-species on H-MFI (90) are also reduced by the reaction, but the spectrum after the reaction is similar to that of Mo_2C. It is summarized that reductive effect of Mo species on H-MFI (90) by the reaction is larger than that on SAH-1, and the difference relate to the catalytic activity. To clarify the differences, second derivatives of their spectra can be evaluated. For MoO_3/SAH-1, only shoulder peak at ca. 2525 eV can be seen, and another components of reduced ions seem to be overlapped at 2528 eV with remained Mo^{6+} ions. It is likely that partially reduced species (without deep reduction to form Mo^{2+} ions) are brought about by the reaction. The components in MoO_3/H-MFI (90) after the reaction are similar to those of Mo_2C, indicating the formation of Mo^{2+}-carbide species in major. However, coexistence of oxo-species is suggested by the results of second derivatives of XANES spectra. It is concluded that formation of dispersed Mo^{2+}-carbide species with oxo-species is a key role for generation of active species.

BL1A

Analysis on Electronic Structures of the Layered and Spinel Oxides

H. Kobayashi[1], I. Teshima[2]

[1]*Research Institute for Ubiquitous Energy Devices, AIST, Ikeda, Osaka, 563-8577 Japan*

[2]*Department of Molecular Science and Technology, Faculty of Engineering, Doshisha University, Kyotanabe, Kyoto, 610-0321 Japan*

Li-containing layered and spinel oxides have been widely studied as the cathode materials of lithium secondary battery. Especially, layered oxide $LiNiO_2$ has been studied as the promising cathode material because of their large reversible capacity of 210 mAh/g in the voltage range 2.5 to 4.3 V. On the other hand, $LiNiO_2$ showed the less thermal stability compared with $LiMn_2O_4$ at high voltage of 4.3 V and decomposed to release oxygen from the structure below 200°C therefore, Al-doped $Li(Ni_{0.8}Co_{0.2})O_2$ has been reported as good candidate for cathode materials. Above mentioned, Al-doping is the effective way to improve the thermal stability of the layered and spinel materials. On the other hand, how the contribution of Al-doping to materials is still ambiguous in these systems. Detailed information on the Al *K*-edge electronic structure is very important in order to improve the thermal properties of these materials and, therefore, the electronic structures of Al-doped layered $LiNi_{0.8}Co_{0.15}Al_{0.05}O_2$, $LiNi_{0.45}Mn_{0.45}Al_{0.10}O_2$, and spinel $Li_{1.08}Mn_{1.84}Al_{0.08}O_4$ materials were investigated in this study.

Experimental

$LiNi_{0.8}Co_{0.15}Al_{0.05}O_2$ and $Li_{1.08}Mn_{1.84}Al_{0.08}O_4$ were supplied from Toda kogyou co. and Dai Nippon Toryou co.. $LiNi_{0.45}Mn_{0.45}Al_{0.10}O_2$ was synthesized in air at 1273 K for 24 h using appropriate molar ratios of $LiOH{\cdot}H_2O$, $M(CH_3COO)_2{\cdot}6H_2O$ (*M*=Ni and Mn), and $AlNO_3$ [1]. Al K-edge spectra were investigated by the total electron yield with KTP crystal (BL1A at UVSOR) measurements.

Results

Figure 1 shows the Al *K*-edge XANES spectra in Al-foil, α-Al_2O_3, AlF_3, and AlN. All the samples have the valence state of 3+ except for Al, but obvious different spectra were observed. This result indicated that Al *K*-edge spectra strongly depended on the anion or structure of materials. The Al *K*-edge XANES spectrum for $LiNi_{0.45}Mn_{0.45}Al_{0.10}O_2$ was observed as shown in Fig. 2, while it was difficult to obtain the spectra with the good S/N ratio for $LiNi_{0.8}Co_{0.15}Al_{0.05}O_2$ and $Li_{1.08}Mn_{1.84}Al_{0.08}O_4$ because of low content of Al in these materials. The peak position and shape of $LiNi_{0.45}Mn_{0.45}Al_{0.10}O_2$ were similar to that of α-Al_2O_3 compared with AlF_3 and AlN. $LiNi_{0.45}Mn_{0.45}Al_{0.10}O_2$ adopted the α-$NaFeO_2$ structure and the chemical composition can be expressed referring to the Wyckoff positions 3*a* and 3*b* with the space group *R3m* as $[Li_{0.92}Ni_{0.08}]_{3a}[Li_{0.08}Mn_{0.45}Ni_{0.37}Al_{0.10}]_{3b}O_2$ by structural analysis. This spectra observed supported that the Al ions in $LiNi_{0.45}Mn_{0.45}Al_{0.10}O_2$ is the valence state of 3+ and occupy the octahedral site in the structure because Al^{3+} ions occupied on the octahedral site in α-Al_2O_3. The TEY method using soft X-ray may give us useful information to understand the origin of battery performance of battery performance.

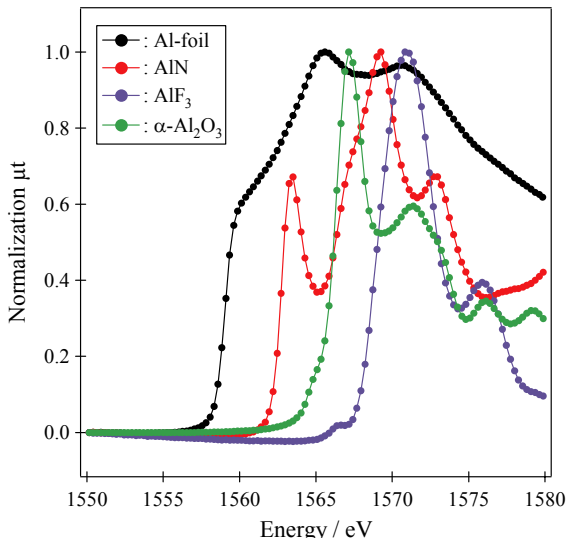

Fig. 1 Al *K*-edge XANES spectra in Al-foil, α-Al_2O_3, AlF_3, and AlN.

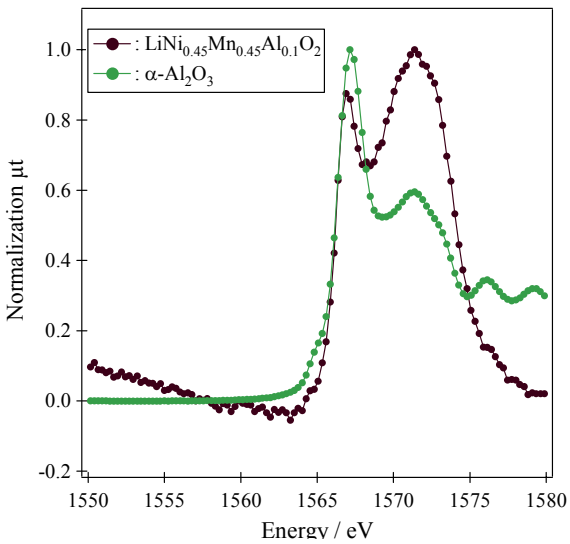

Fig. 2 Al *K*-edge XANES spectra in layered oxide $LiNi_{0.45}Mn_{0.45}Al_{0.10}O_2$ together with α-Al_2O_3.

[1] H. Kobayashi, Y. Arachi, S. Emura, and K. Tatsumi, Solid State Ionics, submitted

BL1A

Characterization of Metal Phtalocyanine by an XAFS Method

T. Kurisaki[1], M. Nasu[1], H. Yamashige[1], H. Wakita[1,2]

[1]*Department of Chemistry, Faculty of Science, Fukuoka University, Nanakuma, Jonan-ku, Fukuoka 814-0180, Japan*

[2]*Advanced Materials Institute, Fukuoka University, Nanakuma, Jonan-ku, Fukuoka 814-0180, Japan*

Phtalocyanines (PC) are synthetic analogues of porphyrins with a structure similar to that of hemoglobin and chlorophyll [1]. The molecular stacking and electronic structure of metallphthalocyanines (MPCs) attract great attention because they exhibit many remarkable capabilities e.g. as catalysts or as one-dimensional or semi-conductors in electronic or opto-electronic devices [2]. But the electronic structure of metallphthalocyanines is not well known.

In this work, we applied X-ray absorption near edge structure (XANES) spectroscopy to two type phtalocyanines, MnPC-Cl and Fe0CP-Cl. The results of the measurement indicate unoccupied and occupied electronic structure of MTPPs. The X-ray absorption spectra were measured at BL1A of the UVSOR in the Institute of Molecular Science, Okazaki [3]. The ring energy of the UVSOR storage ring was 750MeV and the stored current was 110-230 mA. Cl K-edge absorption spectra were recorded in the regions of 2533-3733eV by use of two Ge(111) crystals. The absorption was monitored by the total electron yield using a photomultiplier.

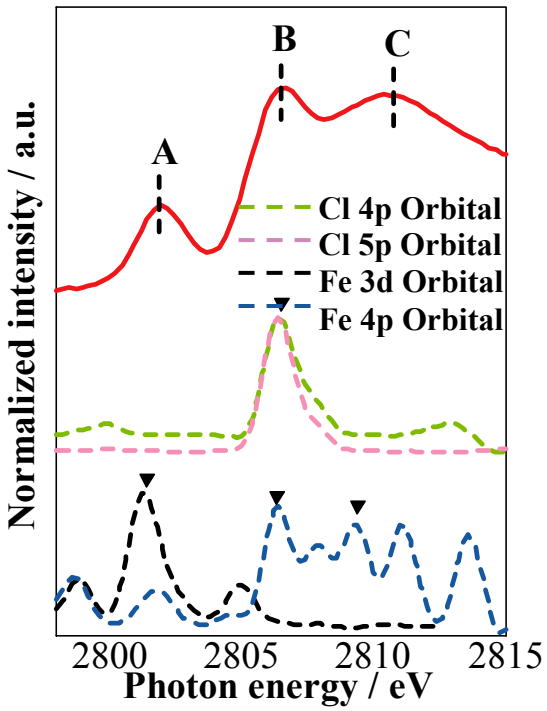

Fig. 1 Observed and calculated Cl K-edge XANES spectra of FePC-Cl.

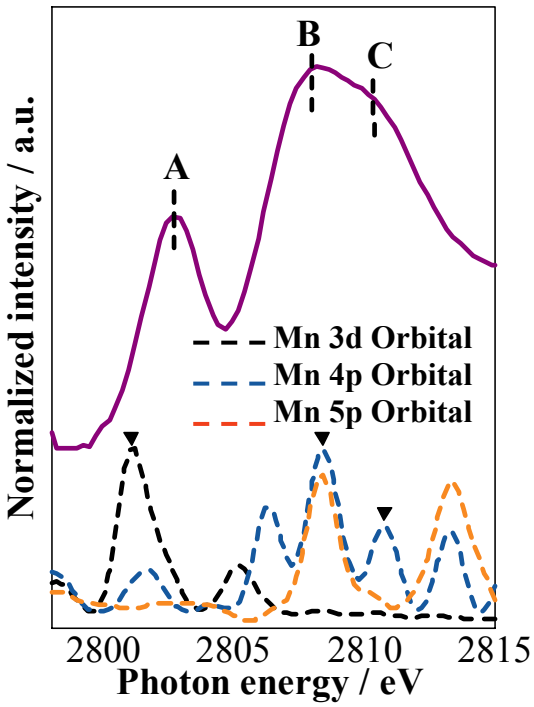

Fig. 2 Observed and calculated Cl K-edge XANES spectra of MnPC-Cl.

The Cl K-edge XANES spectra for the MPCs are shown in Figs. 1 and 2. A remarkable change of the spectral patterns was observed for the MnPC-Cl and FePC-Cl. Comparison of observed and calculated spectra revealed that metal 3d and 4p orbits contribute to peak A and B, respectively. However, MnPC-Cl did not contain contribution from the Cl4p and Cl5p orbits.

[1] F. H. Moser and A. L. Thomas, The phtalocyanines, CRC Press, Boca Raton, FL (1983).
[2] J. Simon F. Tournilhaec and J. –J. André, Nouv. J. Chim., **10** (1986) 295.
[3] S. Murata, T. Matsukawa, S. Naoè, T. Horigome, O. Matsuodo, and M. Watatabe, Rev. Sci. Instrum., **63**, (1992) 1309.

BL1A

Study of Local Structure of S-*K* Edge for Titanium Oxides Synthesized by Anodic Oxidation Treatments

A. Nakahira[1], H. Aritani[2], S. Nakamura[1], H. Nagata[1], H. Murase[1], T. Kubo[1]
[1]*Faculty of Engineering, Osaka Prefecture University, Gakuencho, Sakai 599-8531, Japan*
[2]*Faculty of Engineering, Kyoto Institute of Tech, Matsugasaki, Kyoto 605-8585, Japan*

Various attempts for synthesizing titanium oxide have been carried out by many researchers, since titanium oxide is one of very popular materials for application as a photocatalyst. Usually, the syntheses for titanium oxides have been attempted by sol-gel processings, sputtering, methods, other chemical processings, and vapor phase syntheses. On the contrary, various titanium oxides are able to be synthesize by an anodic oxidation method of titanium metal. This anodic oxidation method is a unique method for preparation of titanium oxides coating on titanium metal. At the same time, this anodic oxidation method is, in addition, considered to be applicable to prepare the high performance titanium oxides, for example, doping some anions in to titanium oxides. Nakahira et al found to be easy to perform by anodic oxidation methods. In the present experiment, titanium oxides was synthesized by anodic oxidation of titanium metal and preparation of titanium oxides doped with S ion was attempted in the mixture of H_2SO_4 solution at various temperatures ranging room temperature and upto 353 K. The evaluation of local structure of S-K edge were performed at BL1A in UVSOR for this S-doped titanium oxides prepared by the anodic oxidation method.

Experiments

In the experiments, titanium metal was used as an anode and carbon black was used as a cathode. The distance between electrodes on anodic oxidation processing was kept to be approximately 3cm. Before anodic oxidation, titanium substrates were polished using abrasive paper, washed with ethanol and finally dried in atmosphere. Ti substrate was soaked in aqueous 0.5M H_2SO_4 solution at room temperature and upto 353 K. Anodic oxidation processing in this study was carried out under a voltage of 80 to 150V supplied with direct current power. For comparison, S-doped TiO_2 were synthesized by heat-treated process at 500°C and its local structure of S was evaluated.

Results and Discussion

From the results by powder X-ray diffraction analysis, the samples obtained by anodic oxidation processing at a voltage of 350V were identified to be anatase, although they possessed relatively broad peaks due to their low crystallinity. Figure 1 shows the results of XANES of S-*K* of some titanium oxides ((a) and (b)) prepared by anodic oxidation in H_2SO_4 solution. Although also the result for S-doped TiO_2 (c) as a reference material was shown, XANES spectra of titanium oxides obtained by anodic oxidation in H_2SO_4 solution were similar to one of S-doped TiO_2 as a reference material. These results of XANES spectra at S-K edge showed that S-doped titanium oxides were successfully prepared by anodic oxidation methods.

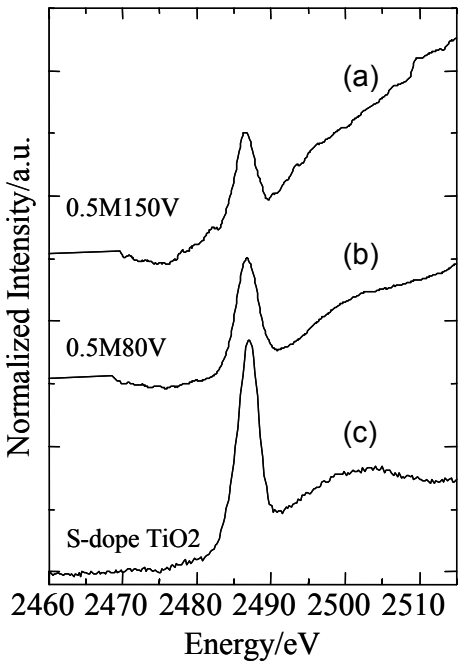

Fig. 1 XANES of S-*K* of some samples prepared by anodic oxidation method.

BL1A

Measurement of Optical Luminescence from a Silica Glass

T. Yoshida[1], S. Obata[1], T. Tanabe[2], H. Yoshida[3]
[1]*Department of Materials, Physics and Energy Engineering, Nagoya University, Furo-cho, Chikusa-ku, Nagoya 464-8603*
[2]*Department of Advanced Energy Engineering Science, Interdisciplinary Graduate School of Engineering Science,Kyushu University6-10-1, Hakozaki, Higashi-ku, Fukuoka 812-8581*
[3]*EcoTopia Science Institute, Nagoya University, Furo-cho, Chikusa-ku, Nagoya 464-8603*

Introduction

Radiation effects on silica glasses are one of the main concerns for their application as optical windows, insulators and optical fibers under fusion and fission environments. The present work is our trial to observe soft X-ray radiation effects on silica. Since the energy region of the soft X-ray covers the K-edges of silicon and oxygen, it is possible to study the dynamic and specific radiation effect of silica under the preferential excitation of these inner-shell electrons. In this study, we have measured the luminescence from silica glasses under the irradiation of soft X-ray near Si K-edge, and discussed the origin and the variation of the luminescence sites.

Experimental

The sample used in this work was an unirradiated low-OH fused silica glasses (T-2030, produced by Toshiba Ceramics, Japan). The diameter and thickness of the sample was 13 mm and 2 mm. The measurement of luminescence of the silica glass induced by soft X-ray irradiation (1.8-1.9 keV) was carried out on the beam line 7A and 1A at UVSOR, Institute for Molecular Science with a stored current of 100-200 mA. The luminescence was focused by a lens in the UHV chamber to the monochromator (CP-200, JOBIN YVON) and detected by a multi-channel analyser (OMA III, EG&G PRINCETON APPLIED RESEARCH). The luminescence yield spectrum was also measured using a photomultiplier (Hamamatsu Photonics R955).

Results and Discussion

Under the irradiation of soft X-rays near Si K-edge, the low-OH fused silica glass (T-2030) showed an intense emission band at around 3.1 eV. Similar luminescence spectra have been measured for silica glasses under in-reactor or UV irradiation [1], and we have concluded that the origins of the present XEOL is likely due to electron excitation of oxygen deficiencies in the silica glass by soft X-ray. Based on the photon energy of the emission bands, the 3.1 eV band should be related to the intrinsic $B_{2\beta}$ center in the low-OH silica glass (T-2030).

We also measured a photoluminescence yield (PLY) spectrum of the 3.1 eV band and showed in Fig. 1(a) together with Si K-edge XANES spectrum (Fig. 1(b)) recorded in the photocurrent mode for the same fused silica glass. One can clearly see that both PLY and XANES spectra are similar, although the former jump negatively whereas the latter positively at Si K-edge. The outline of the phenomenological theory for the shape of the PLY spectrum has been proposed previously [2,3] and is due to the competitive absorption of sites being responsible for the luminescence and those being not. Since in both cases the total absorption condition applies, the key factors that decide the direction of the edge jump are relative luminescence yield of the absorption events above and below the edge. By applying this theory to the present case, above Si K-edge, the transition of Si 1s electron to 3p orbital and/or continuum state occurs and simultaneously the relative luminescence yield reduces; therefore, the PLY spectrum may show the negative and similar feature to XANES spectrum.

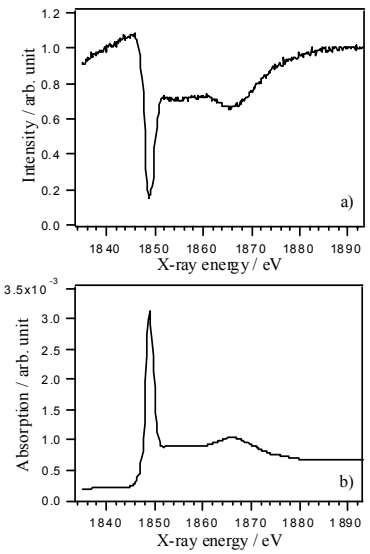

Fig. 1 The comparison between a) the luminescence yield spectrum of the 3.1 eV band and b) Si K-edge XANES spectrum of a fused silica glass.

[1] R. Tohmon *et al*., Phys. Rev. B **55** (1989) 1337.
[2] S. Emura, H. Maeda, M. Nomura, Physica B **208-209** (1995) 108.
[3] T. Murata, D. T. Jiang, T. K. Sham, X. H. Feng, S. P. Frigo, J. Elec. Spectr. Related Phenom. **79** (1996) 155.

BL1A&8B1

Changes in Electronic Structure in $Li_3Fe_2(PO_4)_3$ upon Lithium Insertion

J. Shirakawa[1], M. Nakayama[1], M. Wakihara[1],Y. Uchimoto[2]

[1]*Department of Applied Chemistry, Tokyo Institute of Technology, Tokyo 152-8552 Japan*

[2]*Department of Interdisciplinary Environment, Kyoto University, Kyoto 606-8501, Japan*

Iron oxides with Li insertion sites are attractive for cathode material for lithium ion battery due to their low cost and abundant mine resources. However, Fe^{3+}/Fe^{2+} redox couple usually show only ~ 1.5 V vs. Li^+/Li, indicating smaller energy density than currently used $LiCoO_2$ (~ 3.8 V). In 1997, Padhi *et al.* reported cathode material, $LiFePO_4$ with sufficiently higher voltage, ~ 3.5 V[1]. In this structure, P ions reside in tetrahedral sites and form compact PO_4 polyanion units. These polyanion units form strong covalent bonding, so that the valence electrons of transition metals tend to be isolated from those of polyanions. Such an electronic structure description may relate to its relatively higher voltage.

In this study, we synthesized $Li_3Fe_2(PO_4)_3$ of iron oxide with polyanion units, PO_4, and measured X-ray absorption spectra (XAS) to understand changes in electronic structure upon electrochemical Li insertion.

Experimental

$Li_3Fe_2(PO_4)_3$ was synthesized by a citric acid complex method using $Fe(NO_3)_3{\cdot}9H_2O$, $LiNO_3$ and $NH_4H_2PO_4$ as starting materials. Each starting material with stoichiometric ratio and citric acid was solved into pure water with stirring on the hotplate. After evaporation of solvent, the precursor was sintered twice at 650 ˚C for 12 h, and the targert products were obtained.

X-ray absorption measurements for each element by total electron yield were performed on BL1A (P K-edge) and BL8B1 (Fe L-edge and O K-edge).

Results and Discussion

Electrochemical techniques revealed that lithium insertion took place at around 2.5 V vs Li^+/Li ($x < 1$ in $Li_{3+x}Fe_2(PO_4)_3$), showing higher voltage than conventional Fe^{2+}/Fe^{3+} redox couple. Discharge curve of $Li_{3+x}Fe_2(PO_4)_3$ monotonically varied, indicating topochemical lithium insertion proceeded in the electrochemical reaction.

Figure 1 exhibits the Fe L-edge XAS as a function of Li content in $Li_{3+x}Fe_2(PO_4)_3$. As the Li content increased, absorption peaks shifted to lower energy side, indicating Fe^{3+} reduced to Fe^{2+}. On the other hand, almost no marked change was observed in P K-edge XAS with Li insertion (Figure 2). Thus, P ions did not contribute to charge compensation. O K-edge XAS are presented in Figure 3. Two small peaks are observed at preedge region less than 532 eV, which arise from the hybridization with 3d orbital of iron. These peaks were smaller than commonly known iron oxides, such as FeO and Fe_2O_3, so that the 3d orbital of iron would isolate from the O 2p state. Whereas, the electrochemical lithium insertion led to the increase of their preedge peaks. Thus, changes in electronic structure also took place around oxide ions as well as Fe ions. In addition, this change may accompany the enhancement of hybridization between Fe 3d and O 2p as seen in Fig. 3. To understand the electronic structural change, first-principles calculations for $Li_{3+x}Fe_2(PO_4)_3$ are under progress.

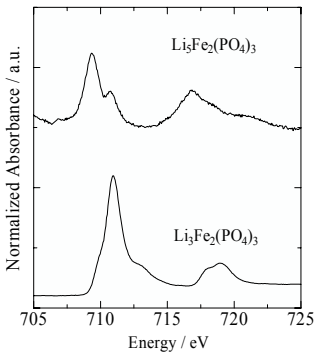

Fig. 1 Fe L-edge XAS of $Li_{3+x}Fe_2(PO_4)_3$.

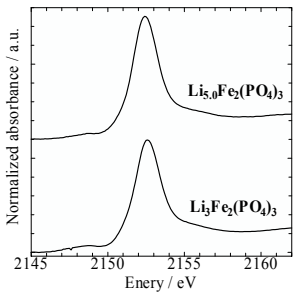

Fig. 2 P K-edge XAS of $Li_{3+x}Fe_2(PO_4)_3$.

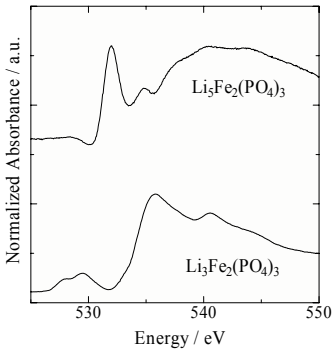

Fig. 3 O K-edge XAS of $Li_{3+x}Fe_2(PO_4)_3$.

[1] Padhi *et al.,* J. Electrochem. Soc. **144** (1997) 1188.

BL5U

Electronic Structure of $CeNiGe_{2-x}Si_x$: Ce 4d-4f Resonant Photoemission Spectroscopy

H.J. Im[1], T. Ito[1,2], S. Kimura[1,2], H.D. Kim[3], J.B. Hong[4], Y.S. Kwon[4]

[1]*School of Physical Sciences, The Graduate University for Advanced Studies, Okazaki 444-8585, Japan*

[2]*UVSOR Facility, Institute for Molecular Science, Okazaki 444-8585, Japan*

[3]*Pohang Accelerator Laboratory, Pohang University of Science and Technology, Pohang 790-784, Korea*

[4]*BK21 Physics Research Division and Institute of Basic Science, Sungkyunkwan University, Suwon 440-746, Korea*

Ce intermetallic compounds have attracted much attention for their various ground states, such as the magnetism, non-magnetic heavy fermion, and quantum criticality. It has been believed that the *cf* - hybridization between the local Ce 4*f* electrons and the itinerant conduction electrons plays an important role to determine these ground states. In this report, we provide a clear understanding of the *cf* - hybridization process by the systematic Ce 4*d*-4*f* resonant photoemission (RPE) study of the isostructural heavy fermion system $CeNiGe_{2-x}Si_x$ ($0 \le x \le 1$), where the ground state originating in Ce 4*f* character varies from an antiferromagnetic regime (AFM, $0 \le x \le 0.8$) to a quantum critical point (QCP, $x = 1$) with increasing Si concentration following a unit volume reduction by about 5 percent [1].

In figure 1 (b), the off-RPE spectra show that the Ni 3*d* peak is located at around 1.8 eV for $x = 0$ and slightly shifts to high-binding energy (around 1.95 eV for $x = 1$) with increasing x in agreement with the LSDA+U (U = 6 eV) band calculation (not shown here). In figure 1 (a), the on-RPE spectra clearly show the two peaks near the Fermi level (E_F): One is Ce $4f^1_{7/2}$ final state at around 0.3 eV, and the other is Ce $4f^1_{5/2}$ final state at E_F, the so-called tail of Kondo resonance peak. The gradual increase of the intensity ratio of Ce $4f^1_{5/2}$ to Ce $4f^1_{7/2}$ peak with increasing Si concentration indicates that the *cf* - hybridization intensity becomes stronger as the ground state of Ce 4*f* electron changes from AFM to QCP.

It is worth comparing the result of $CeNiGe_{2-x}Si_x$ system to that of $CeNi_{1-x}Co_xGe_2$ system where the increase of the *cf* - hybridization comes from the lower binding energy shift of Ni/Co 3*d* state (the intense peak position : 1.8 eV for $x = 0$ and 0.8 eV for $x = 1$) with increasing Co concentration through the QCP ($x = 0.3$) [2,3]. In $CeNi_{1-x}Co_xGe_2$ system, Co substitution gives rise to the simultaneous change of Ni/Co 3*d* density of state and the 3d state character. Therefore, it is difficult to distinguish which effect is more effective. On the other hand, in $CeNiGe_{2-x}Si_x$ system, the increase of hybridization strength with Si substitution is exclusively caused by the increase of chemical pressure due to the reduction of lattice constant without the change of the 3*d* state character. This means that the present system is much suitable for the detection of the *cf*-hybridization effect.

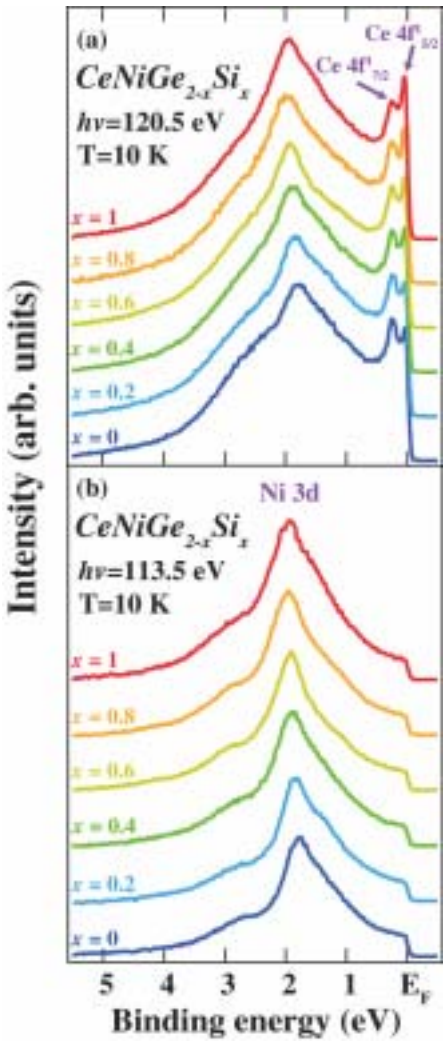

Fig. 1 Ce 4*d*-4*f* on- (a) and off- (b) RPE spectra of $CeNiGe_{2-x}Si_x$.

[1] D.Y. Kim *et al.*, J. Phys. Condens. Matter **16** (2004) 8323.
[2] H.J. Im *et al.*, Phys. Rev. B **72** (2005) 220405(R).
[3] H.J. Im *et al.*, UVSOR Activity Report 2004 (2005) 100.

BL5U

Three-Dimensional Angle-Resolved Photoemission Study on SmS

T. Ito[1,2], H.J. Im[2], A. Chainani[3], K. Matsubayashi[4], S. Kimura[1,2], H.-D. Kim[5], K. Imura[4], H. Suzuki[6], N. K. Sato[4]

[1]*UVSOR Facility, Institute for Molecular Science, Okazaki 444-8585, Japan*

[2]*School of Physical Science, The Graduate University for Advanced Studies, Okazaki 444-8585, Japan*

[3]*RIKEN, SPring-8 Center, Sayo-cho, Sayo-gun, Hyogo 679-5148, Japan*

[4]*Department of Physics, Graduate School of Science, Nagoya University, Nagoya 464-8602, Japan*

[5]*Pohang Accelerator Laboratory, Pohang University of Science and Technology, Pohang 790-784, Korea*

[6]*National Institute for Material Science, Tsukuba, Ibaraki 305-0047, Japan*

SmS is a key material to clarify the physics of strongly correlated electron systems because of its characteristic insulator-metal transition with pressure (~0.7 GPa), so called "black"-"gold" phase transition. In spite of many efforts to understand the origin of its anomalous properties, there is no confidential starting point since the electronic structure has not been clarified. For example, the electrical resistivity [1] as well as the high-resolution photoemission study [2] of "black" SmS suggests the semiconducting gap of Δ~100 meV, while the angle-resolved photoemission spectroscopy (ARPES) has reported wider semiconducting-gap (Δ~400 meV) along (110) emission plane, which has been expected to be the limited tracing points in the Brillouin zone with using He discharge lamp (hν=21.2, 40.8 eV) [3].

To elucidate the intrinsic electronic structure of "black" SmS, especially to clarify the three-dimensional (3D-) electronic structure as well as the semiconducting-gap topology, we have performed 3D-ARPES on "black" SmS.

Figures 1(a) and (b) show the experimental band structures along ΓX and XW lines, respectively. From the estimation of the inner potential V=7 eV, we have mapped out the band dispersion around the exact high-symmetry points [4] with using 3D-ARPES at UVSOR-II BL5U. From the comparison with the previous ARPES, the highly dispersive bands at 3-6 eV have been attribute to S 3*p* bands, while the three non-dispersive features near E_F to Sm^{2+} multiplet structures [3]. It should be noted that the observed clear differences of the Sm-4*f*-dispersions between the Γ (> 100 meV) and X (< 20 meV) points are direct evidence for the existence of three-dimensional lattice effect on "black" SmS.

In Fig. 2, there is no feature from E_F to 400 meV, which has also been confirmed at the all points in the (100) plane (not shown). This strongly indicates the intrinsic nature of wide semiconducting gap on "black" SmS against to the previous expectation [3]. To understand the origin of contradiction between thermodynamic and ARPES experiments, further studies are intended.

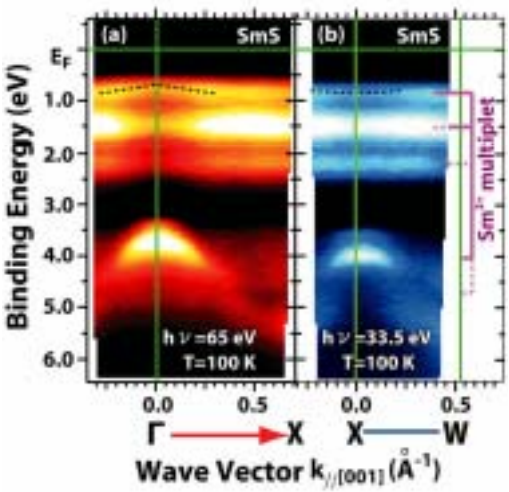

Fig. 1 Experimental band structure of "black" SmS around Γ and X points obtained by present 3D-ARPES. Bright areas correspond to energy bands. Dashed lines are dispersive features of Sm^{2+} multiplets as shown in Fig. 2.

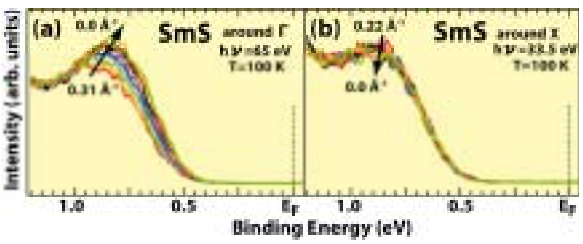

Fig. 2 3D-ARPES spectra near E_F of "black" SmS around Γ (a) and X (b) points, respectively. Arrows indicate the change of ARPES peak positions.

[1] M. Ohashi *et al.*, High Pressure Sci. Technol.**7** (1998) 611.
[2] A. Chainani *et al.*, Phys. Rev. B **65** (2002) 155201.
[3] T. Ito *et al.*, Phys. Rev. B **65** (2002) 155202.
[4] T. Ito *et al.*, Physica B (2006) in press.

BL5U

Three-Dimensional Angle-Resolved Photoemission Study on $CeTe_2$

T. Ito[1,2], H. Im[2], S. Kimura[1,2], Y. S. Kwon[3]

[1]*UVSOR Facility, Institute for Molecular Science, Okazaki 444-8585, Japan*

[2]*School of Physical Sciences, The Graduate University for Advanced Studies, Okazaki 444-8585, Japan*

[3]*BK21 Physics Research Division and Institute for Basic Science, Sungkyunkwan University, Suwon 440-746, Korea*

Anomalous electronic/magnetic properties, such as charge/spin density wave formation, high-Tc superconductivity, etc., have intimate relation with the anisotropic electronic/magnetic structure of materials. Thus, it is important to understand the effect of the low-dimensional electronic structure relates to the unconventional physical properties. On the other hand, the most of studies on the low-dimensional compounds persist on the standing point of ideal two- or one-dimensional case, though the sizable three-dimensionality on the real system has essential relation with its anomalous properties.

To show the importance of three-dimensionality at the electronic structure correlating with the anomalous physical properties, we have performed three-dimensional angle-resolved photoemission spectroscopy (3D-ARPES) [1] on $CeTe_2$, which crystallizes in the layered structure formed by the planar Te(1) sheet sandwiched by the corrugated CeTe(2) double layers [2].

Figure 1 shows the Fermi surface image along ΓZMR plane of $CeTe_2$ obtained by plotting the ARPES intensity integrated from the Fermi level (E_F) to 100 meV binding energies. Yellow and red areas correspond to the Fermi surface. In Fig. 1, the Brillouin zone boundaries have been estimated from the symmetry of band dispersions along ΓZ line (Fig. 2(a)) obtained by utilizing the energy vs momentum relation of $k_{\perp} = (2\pi/h)\sqrt{2mE_k\cos^2\theta + V}$, where E_K is kinetic energy at E_F, θ=0°, and V is inner potential, which is slightly larger (V~16.4 eV) than the previous report (V~15 eV) [3], possibly due to the insufficient photon energy range on the previous estimation.

From the comparison with the band calculation [4], two Fermi surfaces around ΓZ axis (dashed lines) originating in hole-like FS with Te(1) character, whose two-dimensionality is roughly consistent with the anisotropic crystal structure as well as thermodynamic properties [2].

On the other hand, we have observed broad features (purple dashed lines in Fig. 2(a)) that indicate "band folding" along ΓZ lines. This strongly suggests the three-dimensional electronic structure on $CeTe_2$. We believe that the observed three-dimensionality can be ascribed as the existence of 3D nesting vector, which has not been reported so far [4,5]. The present results clearly show the future aspect of the 3D-ARPES as a tool for the study of the low-dimensional strongly correlated electron systems.

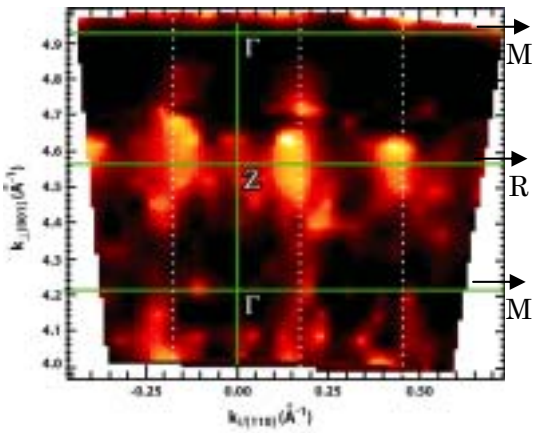

Fig. 1 Fermi surface mapping on ΓZMR plane of $CeTe_2$ obtained by 3D-ARPES. Dashed lines are guide for eyes.

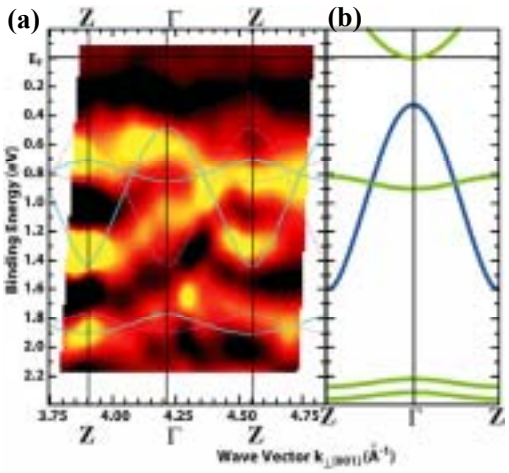

Fig. 2 (a) Band structure along ΓZ line of $CeTe_2$ obtained by 3D-ARPES. Solid and dashed lines are guide for eyes. (b) Band calculation of $CeTe_2$. Green and blue lines correspond to the bands on Te(1) and CeTe(2) layer, respectively.

[1] J. Schäfer *et al.*, Phys. Rev. B **72** (2005) 155115.
[2] M. H. Jung *et al.*, Phys. Rev. B **62** (2000) 11609.
[3] T. Ito *et al.*, UVSOR Activity Report 2004, 99; Physica B, in press.
[4] J. H. Shim *et al.*, Phys. Rev. Lett. **93** (2004) 156406.
[5] K.Y. Shin *et al.*, Phys. Rev. B **72** (2005) 085132.

BL5U

3*p*-3*d* Resonance Photoemission Spectroscopy of Heusler-Type $Fe_2VAl_{1-z}Si_z$

H. Miyazaki[1], M. Inukai[1], S. Ota[1], T. Suzuki[1], M. Kato[1], S. Yagi[1], K. Soda[1]
Y. Nishino[2], T. Ito[3], S. Kimura[3]
[1]*Graduate School of Engineering, Nagoya University, Nagoya 464-8603 Japan*
[2]*Graduate School of Engineering, Nagoya Institute of Technology, Nagoya 466-8555 Japan*
[3]*UVSOR Facility, Institute for Molecular Science, Okazaki 444-8585 Japan*

Introduction

Heusler-type Fe_2VAl and related alloys such as $Fe_2VAl_{1-z}Si_z$ have attracted much attention because of not only scientific interest in their anomalous transport properties [1] but also potential application for thermoelectric materials [2]. In order to clarify the origin of the fascinating transport and thermoelectric properties, we have investigated the electronic structure of $Fe_2VAl_{1-z}Si_z$ alloys by photoelectron spectroscopy. In this paper, we will report results of the Fe and V 3*p*-3*d* resonance photoemission study.

Experimental

Photoelectron spectra of polycrystalline specimens of $Fe_2VAl_{1-z}Si_z$ alloys were recorded under 2.7×10^{-8} Pa at 30 K with a high-resolution energy analyzer at BL5U. The origin of the binding energy E_B, the Fermi level (E_F), and the total energy resolution were determined by the measurement of the Fermi edge of an evaporated gold film. The total energy resolution was 45 meV at the excitation photon energy of 50 eV. Clean surfaces for the photoelectron measurement were prepared by in-situ fracturing the specimens.

Results and Discussion

Figures 1 and 2 show the Fe and V 3*d* states, respectively, of $Fe_2VAl_{1-z}Si_z$ estimated from the resonance photoemission spectroscopy as well as their partial densities of states theoretically calculated for Fe_2VAl. The overall features of the Fe and V 3*d* states agree considerably well with the respective partial densities of states, although there is the large intensity near E_F attributed to the surface states appearing in the pseudo-gap [3] and the V 3*d* states are located in lower binding energy than expected.

As the Si substitution *z* is increased from 0 to 0.05, the Fe 3*d* states show almost no change in the main peak position but the intensity decrease in the low energy side of the peak. With *z* increased to 0.10, the Fe 3*d* states are again enhanced between E_B of 0.5 eV and E_F. The hump around E_B = 2.5 eV seems to move to the low binding energy side. On the other hand, the V 3*d* states, in particular the V t_{2g} peak at E_B ~ 1.3 eV, are shifted gradually to the high binding energy side as *z* increases, but the contribution is reduced near E_F. Since it is expected that the V 3*d* t_{2g} states are not so much hybridized with the Al and Si *sp* states, the shift of the V t_{2g} states imply the increase in the electrons at the V site on the substitution, which is consistent with the observation of the V 2*p* core level shift.

The present findings indicate the non-rigid band -like change in the electronic structure induced by the Si substitution. However, the observed dependence of the thermoelectric power [2] is explainable by the observation, *i.e.* the shift of the V 3*d* states and the intensity decrease at E_F at $z = 0.05$ and the emergence of the Fe 3*d* states in the pseudo-gap at $z = 0.10$.

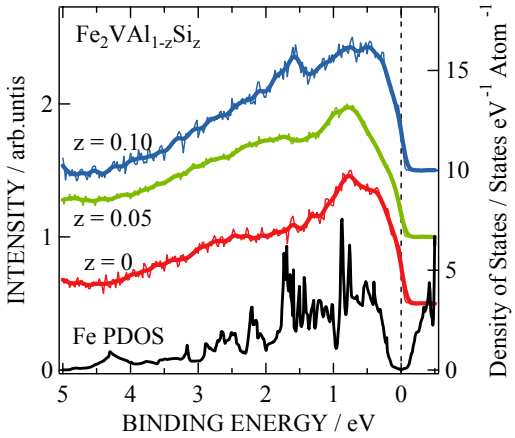

Fig. 1 Energy distribution of the Fe 3*d* states of $Fe_2VAl_{1-z}Si_z$. The theoretical density of the Fe 3*d* states (Fe PDOS) of Fe_2VAl is also shown for comparison.

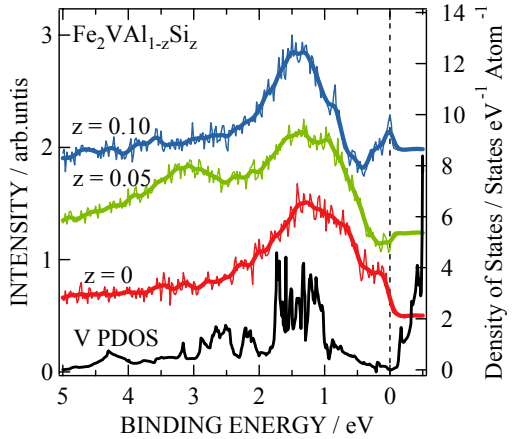

Fig. 2 Energy distribution of the V 3*d* states of $Fe_2VAl_{1-z}Si_z$. The theoretical density of the V 3*d* states (V PDOS) of Fe_2VAl is also shown for comparison.

[1] Y. Nishino *et al.*, Phys. Rev.Lett. **79** (1997) 1909.
[2] H. Kato *et al.*, J. Jpn. Inst. Metals **65** (2001) 652.
[3] K. Soda *et al.*, Phys. Rev. B **71** (2005) 245112.

BL5U

Angle-Resolved Photoemission Spectroscopy of Heusler-Type Fe_2VAl

H. Miyazaki[1], M. Inukai[1], S. Ota[1], T. Suzuki[1], M. Kato[1], S. Yagi[1], K. Soda[1]
K. Fukuda[2], Y. Yamada[3], T. Ito[4], S. Kimura[4]
[1]*Graduate School of Engineering, Nagoya University, Nagoya 464-8603 Japan*
[2]*Graduate School of Science and Technology, Niigata University, Niigata 950-2181 Japan*
[3]*Department of Physics, Niigata University, Niigata 950-2181 Japan*
[4]*UVSOR Facility, Institute for Molecular Science, Okazaki 444-8585 Japan*

Introduction

A Heusler-type Fe_2VAl intermetallic compound has attracted much attention because of its unusual transport properties [1]: the semiconductor-like temperature dependence of the electric conductivity, the enhancement of the effective electron mass at low temperatures and a marginally magnetic property. Furthermore, the small deviation of its composition from the stoichiometry causes the drastic increase of the electric conductivity at low temperatures and the unexpected enhancement of the thermoelectric power. According to a band structure calculation [2], Fe_2VAl is a non-magnetic semimetal with a sharp pseudo-gap right at the Fermi level E_F. However, the origin of the unusual transport properties has not been clarified yet. Thus we have experimentally investigated the band structure of Fe_2VAl by the angle-resolved photoemission spectroscopy (ARPES).

Experimental

The ARPES measurements were carried out at BL5U under 2.7×10^{-8} Pa at 25 K. The origin of the binding energy E_B, *i.e.* E_F was determined by measuring the Fermi edge of an evaporated Au film. The total energy resolution was also estimated by the Fermi edge to be 0.13 eV at the excitation photon energy $h\nu$ of 87 eV and 0.045 eV at $h\nu$ = 47 eV. The angle resolution was set to 0.5°. Clean surfaces of single crystalline Fe_2VAl were prepared by *in situ* fracturing them in parallel to a (111) surface.

Results and Discussion

Figures 1 and 2 show the valence band structures of Fe_2VAl, which were obtained from the second derivative of the normal ARPES spectra and the off-normal ones recorded at $h\nu$ = 47 eV, respectively. We have distinguished at least five bands labeled as A to D in Fig.1 and A' to E' in Fig.2, as shown by white curves as guides for eyes. Black curves indicate the band structure calculated by the code WIEN 2K [3], which is consistent with that reported so far [2].

The A (A') and B (B') bands form small electron pockets around the Γ and L ($\bar{M}$) points, respectively. The A (A') and D (D') bands agree fairly well with the calculated ones. The C band may be attributed to a surface state, showing no dispersion along the surface normal. The present normal ARPES study also suggests that the surface state might be derived from the V 3*d* states, since $h\nu$ for the Γ point corresponds to the V 3*p* threshold region. According to the calculation and the 3*p*-3*d* resonance photoemission study for polycrystalline alloys [2,4], the main V 3*d* band is located at E_B ~ 1.3 eV, which may be suppressed because of the selection rules. Detailed analysis and further study for non-stoichiometric compounds $Fe_{2-x}V_{1+x}Al$ will be reported elsewhere.

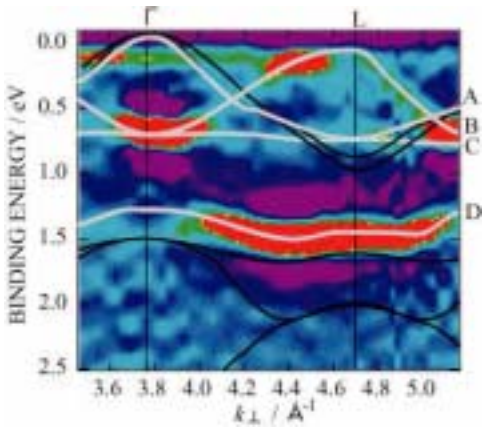

Fig. 1 Valence band structure of Fe_2VAl obtained by the normal ARPES of a (111) surface.

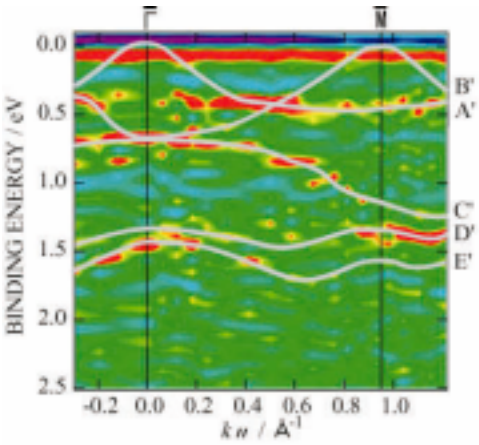

Fig. 2 Valence band structure of Fe_2VAl obtained by the off-normal ARPES of a (111) surface.

[1] Y. Nishino *et al.*, Phys. Rev. B**71** (2005) 094425.
[2] G. Y. Guo *et al.*, J. Phys.:Condens. Matter **10** (1998) 119.
[3] P. Blaha *et al.*, Compt. Phys. Commun. **59** (1990) 399.
[4] H. Miyazaki *et al.*, *in the present Activity Report.*

BL5U

Electronic Structure of Heusler-Type $(Fe_{1-x}M_x)_2VAl$ (M=Ir, Pt)

T. Mochizuki[1], H. Miyazaki[2], M. Kato[2], S. Yagi[2], K. Soda[2],
A. Miyashita[3], Y. Nishino[3], T. Ito[4], S. Kimura[4]
[1]*School of Engineering, Nagoya University, Nagoya 464-8603, Japan*
[2]*Graduate School of Engineering, Nagoya University, Nagoya 464-8603, Japan*
[3]*Graduate School of Engineering, Nagoya Institute of Technology, Nagoya 466-8555 Japan*
[3]*UVSOR, Institute for Molecular Science, Okazaki 444-8585 Japan*

Introduction

Heusler-type Fe_2VAl and its related alloys have received much attention because Fe_2VAl possesses a sharp pseudogap across the Fermi level E_F and shows the remarkable enhancement of thermoelectric properties by the partial substitution [1]. To develop new thermoelectric materials, it is important to clarify how the electronic structure is changed by the partial substitution. In this report, we will show the results of the 3*p*-3*d* resonance photoemission measurement of Heusler-type alloys $(Fe_{1-x}M_x)_2VAl$ (M=Ir, Pt).

Experimental

Samples are polycrystalline of the Heusler-type $(Fe_{0.98}Ir_{0.02})_2VAl$, $(Fe_{0.99}Pt_{0.01})_2VAl$ and Fe_2VAl in a size of 1x1x5 mm^3. Photoelectron spectra were recorded under $2.7x10^{-8}$ Pa at 30 K at BL5U. Clean surfaces were prepared by the in-situ fracture.

Results and Discussion

Observed valence-band spectra show three features at the binding energy E_B of 0.8, 1.4 and 3.0 eV. The overall features agree well with the bulk-sensitive soft X-ray photoelectron spectra (XPS) of Fe_2VAl [2] except for the feature around E_F. The large intensity at E_F in the present spectra for Fe_2VAl suggests the surface states appearing in the pseudogap. By the partial substitution of Ir or Pt for Fe, the intensity at E_F is reduced and the peak at E_B = 1.3 eV is shifted to the high binding energy side.

Figures 1 and 2 show partial densities of the Fe and V 3*d* states, respectively, estimated from the relevant 3*p*-3*d* resonance photoemission. With the partial substitution, the Fe 3*d* states are reduced at E_F and the hump around 2.5 eV seems to be shifted for $(Fe_{0.98}Ir_{0.02})_2VAl$ and split for $(Fe_{0.99}Pt_{0.01})_2VAl$, as shown by arrows, while the V 3*d* peak at E_B = 1.3 eV is shifted to the higher binding energy and a new peak, indicated by an arrow, appears at the low binding energy side of the peak. These changes can be explained by the large *d*-*d* interaction of Ir and Pt with Fe and V and the relative energy position of their *d* states [3], although the surface contribution is not so clear at present. The present study also suggests that the enhancement of the thermoelectric power by the substitution may be caused by the shift of the V 3*d* band and the reduction of the Fe 3*d* states near E_F.

Detailed analysis with a theoretical calculation and further study of the spectral dependence on the amount of the substitution *x* are now in progress.

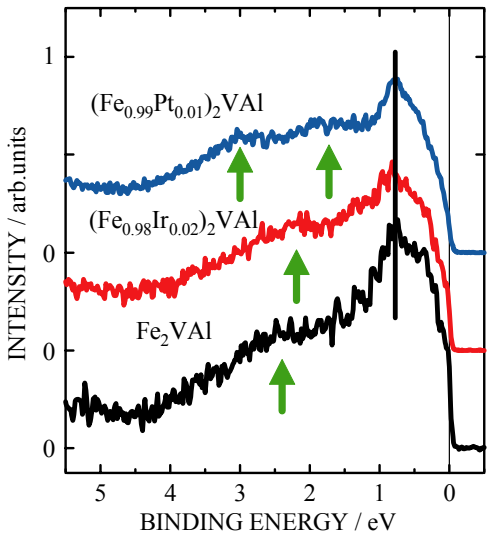

Fig. 1 Partial density of the Fe 3*d* states of $(Fe_{0.98}Ir_{0.02})_2VAl$, $(Fe_{0.99}Pt_{0.01})_2VAl$ and Fe_2VAl.

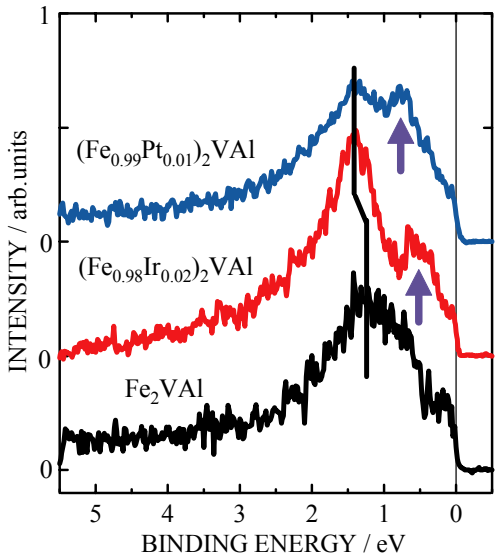

Fig. 2 Partial density of the V 3*d* states of $(Fe_{0.98}Ir_{0.02})_2VAl$, $(Fe_{0.99}Pt_{0.01})_2VAl$ and Fe_2VAl.

[1] Y. Nishino *et al.*, Mater. Sci. Forum **449-452** (2004) 909.
[2] K. Soda *et al.*, Phys. Rev. B, **71** (2005) 245112.
[3] W. A. Harrison, Electronic Structure and The Properties of Solids, (W. H. Freeman & Co., San Francisco, 1989).

BL5U

Electronic Structure of Pd-TM-P (TM = Ni, Cu) Bulk Metallic Glasses

S. Ota[1], T. Suzuki[1], H. Miyazaki[1], K. Soda[1],
T. Wada[2], M. Hasegawa[2], N. Nishiyama[3], T. Ito[4], S. Kimura[4]
[1]*Graduate School of Engineering, Nagoya University, Nagoya 464-8603 Japan*
[2]*Institute for Materials Research, Tohoku University, Sendai 980-8577 Japan*
[3]*R&D Institute of Metals and Composites for Future Industries, Sendai 980-8577 Japan*
[4]*UVSOR, Institute for Molecular Science, Okazaki 444-8585 Japan*

Introduction

Recently, the bulk metallic glasses (BMG's) have received much attention as a new material possessing excellent mechanical, physical and chemical properties. It is important for developing a new functional BMG to understand the mechanism of the BMG's phase stability from the microscopic point of view. The Pd-based BMG has the large glass formation ability and is one of promising structural materials. Here, we have studied the electronic structure of the Pd-based BMG by use of synchrotron radiation photoelectron spectroscopy (PES).

Experimental

The PES experiment was carried out at BL5U under 2 x 10^{-8} Pa at 20 K. Total energy resolution was 40 meV at the excitation photon energy $h\nu$ of 40 eV. BMG specimens were $Pd_{40}Ni_{40}P_{20}$, $Pd_{50}Cu_{30}P_{20}$ and $Pd_{42.5}Cu_{30}Ni_{7.5}P_{20}$, and their clean surfaces were prepared by in situ scraping them with a diamond file.

Result and Discussions

Figure 1 shows valence-band photoelectron spectra of $Pd_{42.5}Cu_{30}Ni_{7.5}P_{20}$ recorded with the various photon energies $h\nu$, which are indicated in the figure. They are normalized by the intensity integrated up to 11 eV. There are three structures found at the binding energies E_B of 2.3, 2.8 and 3.7 eV. The structure at E_B = 2.8 eV becomes prominent at $h\nu$ = 85 eV and those at E_B of 2.3 and 3.7 eV are distinguished at the low excitation photon energy. These are consistent with the reported results [1].

Spectra of $Pd_{50}Cu_{30}P_{20}$ and $Pd_{40}Ni_{40}P_{20}$ are shown in Fig.2. The spectra of $Pd_{50}Cu_{30}P_{20}$ reveals three structures similar to $Pd_{42.5}Cu_{30}Ni_{7.5}P_{20}$, while another band appears at E_B = 0.7 eV for $Pd_{40}Ni_{40}P_{20}$, in particular at the high excitation photon energy.

The calculated photoionization cross section of Pd 4*d* states shows a maximum at $h\nu$ ~ 35 eV and the Cooper minimum at $h\nu$ ~ 110 eV, and those of Ni and Cu 3*d* states change gradually [2]. Thus, the 0.7- and 2.8-eV bands are attributed to the Ni and Cu 3*d* states, respectively. On the other hand, the 2.3-eV band is noticeable at the low photon energy and the 3.7-eV band at $h\nu$ ~ 50 eV. This $h\nu$-dependence suggests that the 2.3- and 3.7-eV bands may be derived from the P 3*p* and Pd 4*d* states, respectively.

These assignments agree well with the results of the soft x-ray emission and hard x-ray PES measurements [3], the latter of which shows another band at E_B ~ 6.3 eV, indicating the P 3*s* states. The Pd 4*d* and P 3*p* states also seems to extend from E_B ~ 4 to 2 eV, which might imply a Pd-P covalent bond as in a structural unit Pd_3P reported for $Pd_{40}Ni_{40}P_{20}$ [4].

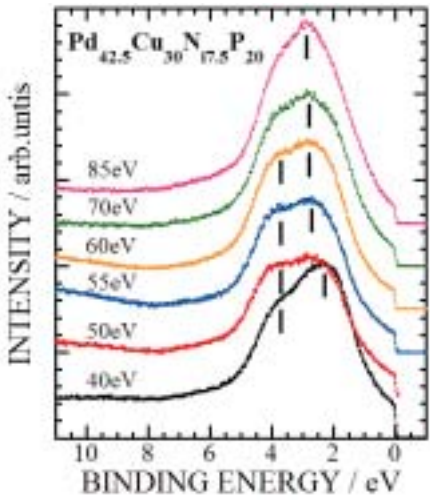

Fig. 1 Valence-band spectra of $Pd_{42.5}Cu_{30}Ni_{7.5}P_{20}$.

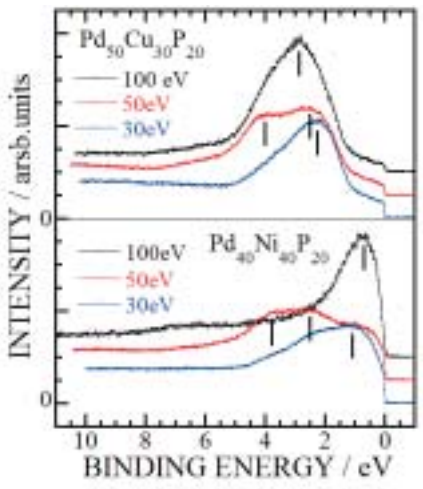

Fig. 2 Valence-band spectra of $Pd_{50}Cu_{30}P_{20}$ and $Pd_{40}Ni_{40}P_{20}$.

[1] S. Hosokawa *et al*., Mat. Trans. **46** (2005) 2803.
[2] J. J. Yeh and I. Lindau, Atomic Data and Nucl. Data Tables **32** (1985) 1.
[3] S. Ota *et al*., *unpublished*.
[4] T. Otomo *et al*., Physica B **213&214** (1995) 529.

BL5U

Electronic Structure of Zr-TM-Al (TM = Ni, Cu) Bulk Metallic Glasses II

T. Suzuki[1], H. Miyazaki[1], S. Ota[1], M. Inukai[1], M. Kato[1], S. Yagi[1], K. Soda[1]
M. Hasegawa[2], T. Takeuchi[3], H. Sato[4], U. Mizutani[5], T. Ito[6], S. Kimura[6]
[1]*Graduate School of Engineering, Nagoya University, Nagoya 464-8603, Japan*
[2]*Institute for Materials Research, Tohoku University, Sendai 980-8577, Japan*
[3]*Ecotopia Science Institute, Nagoya University, Nagoya 464-8603, Japan*
[4]*Aichi University of Education, Kariya 448-8542, Japan*
[5]*Toyota Physical and Chemical Research Institute, Nagakute-cho, Aichi-gun 480-1192, Japan*
[6]*UVSOR, Institute for Molecular Science, Okazaki 444-8585, Japan*

Introduction

Bulk metallic glasses (BMG's) show the large glass formation ability and the physical, chemical and mechanical properties which are superior to crystalline materials [1]. In order to understand the origin of their phase stability from the microscopic point of view, we have systematically studied the electronic structure of the Zr-based BMG's, Zr-TM-Al (TM = Ni, Cu), with use of photoelectron spectroscopy.

Experimental

Photoelectron spectra were recorded under 2x10^{-8} Pa at 25 K at BL5U. Total energy resolution and the origin of the binding energy E_B, *i.e.* the Fermi level E_F, were determined by the Fermi edge of an evaporated Au film.

Specimens were ternary $Zr_{66.7}Cu_{25.8}Al_{7.5}$, $Zr_{50}Cu_{35}Al_{15}$, $Zr_{65}Ni_{25}Al_{10}$, $Zr_{65}Ni_{20}Al_{15}$ and quaternary $Zr_{55}Cu_{35}Ni_5Al_{10}$ BMG's in a size of ϕ2 mm x 3 mm. Clean surfaces for the photoelectron measurement were prepared by *in situ* scraping the specimen with a diamond file.

Results and Discussions

Figure 1 shows typical valence-band spectra recorded at the excitation photon energy $h\nu$ of 40.5 eV. They are normalized by the intensity integrated up to the binding energy E_B of 10 eV. Three bands at E_B ~ 0.6, 2.0 and 3.5 eV are ascribed to the Zr 4*d*, Ni 3*d* and Cu 3*d* bands, respectively. For Zr-Cu-Al, the peak of the Zr 4*d* band, indicated by an arrow, is located at the higher binding energy with the supercooled liquid region $\Delta T_x = T_x - T_g$ (T_x: crystallization temperature, T_g: glass transition temperature) increased. This may suggest that the large resistance to the crystallization is induced by the formation of the Zr 4*d* chemical bond. However, Zr-Ni-Al shows almost no change in the Zr 4*d* peak.

The spectrum recorded at $h\nu$ = 21.2 eV shows the intensity reduction near E_F, *i.e.* the existence of a pseudogap [2,3], which implies the decrease in the internal energy of the electron system in the BMG. In Fig.2, the width ΔE_g of the pseudogap, estimated by the spectrum, is plotted as a function of one of the parameters representing the BMG's stability, the ratio T_g/T_l. Here, T_l is the liquidus temperature. As the ratio T_g/T_l increases, indicating that the BMG's can be made easily from the melt, ΔE_g is increased for Zr-Ni-Al but decreased for Zr-Cu-Al. This difference may be related to the fact that the maximum of ΔT_x nearly coincides with the maximum of T_g/T_l in the phase diagram for Zr-Ni-Al, while ΔT_x reveals two local maxima at the compositions of the present Zr-Cu-Al specimens.

Further systematic study is in progress for the Zr-Ni-Al and Zr-Cu-Al BMG's with different compositions.

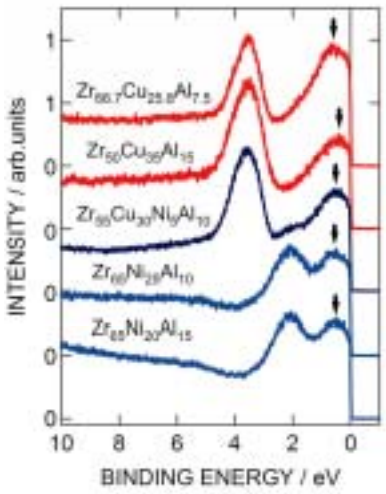

Fig. 1 Valence-band spectra of Zr-TM-Al (TM = Ni, Cu) recorded at $h\nu$ = 40.5 eV.

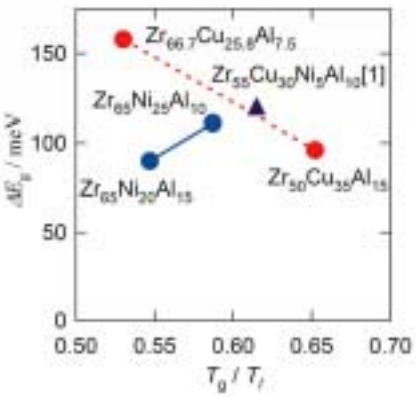

Fig. 2 Relation between the width of the pseudogap ΔE_g and the ratio T_g/T_l.

[1] M. Telford, Mater. Today **7** (2004) 36.
[2] T. Suzuki *et al*. J. Jpn. Soc. Powder Powder Metallurgy **53** (2006) 107.
[3] K. Soda *et al*., J. Electron Spectrosc. Relat. Phenom. **144-147** (2005) 585.

BL5U

Pseudogap Formation in the Density of States of Relevant Crystals of the Zr-Ni-Al Bulk Metallic Glass

T. Takeuchi[1,2], S. Nakano[2], T. Kitao[2], H. Kaga[2], T. Ito[3], S. Kimura[3]
[1]*EcoTopia Science, Institute, Nagoya University, Nagoya 464-8603 Japan*
[2]*Department of Crystalline Materials Science, Nagoya University, Nagoya 464-8603 Japan*
[3]*UVSOR Facility, Institute for Molecular Science, Okazaki 444-8585 Japan*

Recent discovery of the amorphous phase capable of forming in bulk-shape has attracted a great deal of interests because of their ability in practical usage, such as mechanical parts of high strength, surface coating materials with high degree of hardness, and soft-magnetic material. These amorphous phases are widely known as the Bulk Metallic Glass (BMG). In order to utilize the BMG's as practical materials, one should gain deep insight into their stabilization mechanism.

The formation of a pseudogap at the Fermi level (E_F) has been discussed as one of the factors to reduce the internal energy of the BMG's. This effect was firstly discussed by Nagel and Tauc [1], and then studied intensively both experimentally [2] and theoretically [3][4]. Nagel and Tauc used a model with a nearly-free-electron gas and employed perturbation theory, in which structure factor $S(q)$ plays an important role in altering eigen values of the conduction electrons. A peak in $S(q)$ at particular q_p produces a pseudogap in the density of states $N(E)$ at $E_{PG} = \hbar^2 q_p^{\,2} / (8m_e)$. If the condition E_F=E_{PG} is satisfied, the population of the conduction electrons around the highest energy is effectively suppressed and the total kinetic energy of electrons is reduced to stabilize the structure.

A resonance between the conduction electrons with the local atomic arrangements would produce the experimentally observed pseudogap in the BMG. One may expect that the relevant crystals possessing the same local atomic arrangements could have the similar pseudogap in their electronic density of states at E_F. Thus it is of great importance to investigate the pseudogap formation not only of the BMG's but also of their relevant crystals to gain insight into its contribution to the BMGs' stability. In this study, therefore, we investigated electronic structure near E_F of the relevant crystals using the high-resolution ultraviolet photoemission spectroscopy.

Figure 1 shows high-resolution UPS spectra near E_F of the Zr_6NiAl_2, ZrNiAl, Zr_5Ni_4Al, and ZrNi. All the intermetallic compounds except for the Zr_5Ni_4Al were already confirmed to possess the local atomic clusters constituting the BMG. [5] Only the structure of Zr_5Ni_4Al has not been determined yet, and therefore, we were not able to know its local atomic arrangements. We employed it in the present UPS measurements because the Zr_5Ni_4Al is stabilized in the vicinity of the composition area of the BMG's and may have the similar local atomic arrangements as those in the BMG's.

Obviously the UPS spectra of all relevant crystals possess a pseudogap of a few hundred meV in width. [6] The energy width of these pseudogaps is comparable with that reported for the Zr-Ni-Cu-Al BMG.[4] Thus it is argued from the present UPS measurements that the characteristic local atomic arrangements could produce the pseudogap formation, and that the resulting pseudogap does effectively reduce the internal energy of the BMG's and their relevant crystals.

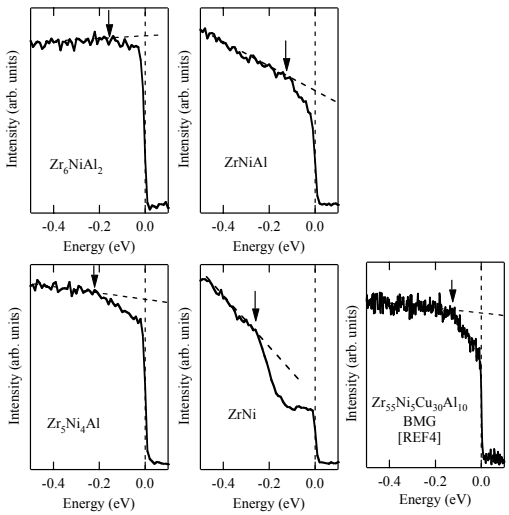

Fig. 1 (a)-(d) High-resolution UPS spectra near E_F of the relevant crystals. UPS spectrum of the corresponding BMG is also shown in the panel (e).

[1] S. R. Nagel, J. Tauc, Phys. Rev. Lett. **35** (1975) 380.
[2] For example, U. Mizutani, K. T. Hartwig, T. B. Massalski, Phys. Rev. Lett. **41** (1978) 661.
[3] For example, D. Nicholson, L. Schwartz, Phys. Rev. Lett. **49** (1982) 1050-1053., J. Hafner, Phys. Rev. B **21** (1980) 406.
[4] K. Soda, K. Shimba, S. Yagi, M. Kato, T. Takeuchi, U. Mizutani, T. Zhang, M. Hasegawa, A. Inoue, T. Ito, S. Kimura, J. Elec. Spec. Relat. Phenom. **144-147** (2005) 585.
[5] T. Takeuchi, S. Nakano, K. Soda, H. Sato, M. Hasegawa, U. Mizutani, K. Itoh, T. Fukunaga, Mat. Trans **46** (2005) 2791.
[6] T. Takeuchi, S. Nakano, K. Soda, H. Sato, M. Hasegawa, U. Mizutani, K. Itoh, T. Fukunaga, submitted to Materials Science and Engineering A (2005) August.

BL5U

Synchrotron-Radiation Photoemission Study of Alkyl-Passivated Si Nanoparticle

A. Tanaka[1, 2, 3], R. Saito[2, 4], T. Kamikake[2], M. Imamura[3]

[1]*Department of Mechanical Engineering, Faculty of Engineering, Kobe University, Kobe 657-8501, Japan*

[2]*Department of Mechanical Engineering, Graduate School of Science and Technology, Kobe University, Kobe 657-8501, Japan*

[3]*Department of Mechanical and Systems Engineering, Graduate School of Science and Technology, Kobe University, Kobe 657-8501, Japan*

[4]*Department of Physics, Graduate School of Science, Tohoku University, Sendai 980-8578, Japan*

Semiconductor nanoparticles are attracting much interest from the viewpoint of both fundamental and device physics, since they show the distinctive physical and chemical properties found in neither bulk nor molecular/atomic systems. Especially, the various Si nanostructures have a great interest, since it has been reported that they show a strong photoluminescence [1]. However, their optical properties depend on the samples in the literatures. In order to understand the intrinsic properties of these Si-based nanostructured materials, it is indispensable to prepare the well- defined samples and investigate their intrinsic electronic structures. In this work, we have carried out a systematic synthesis and the various spectroscopic studies of alkyl-passivated Si nanoparticles in order to characterize their intrinsic optical properties and electronic structures.

The synthesis procedure of alkyl-passivated Si nanoparticles used in this work is described elsewhere [2]. Photoemission measurements of alkyl-passivated Si nanoparticles on the HOPG substrates were performed at BL5U of UVSOR II Facility. The optical spectroscopic measurements of these alkyl-passivated Si nanoparticles were also performed at Kobe University.

The photoluminescence (PL) spectrum of butyl-passivated Si nanoparticle with mean diameter less than 3 nm exhibits a strong emission around 3.7 eV in photon energy. Moreover, the optical extinction spectrum exhibits an absorption edge around 4 eV in photon energy, and the PL excitation (PLE) spectrum also exhibits a distinct resonance around 4 eV in photon energy. In order to investigate the detailed electronic structure of this butyl-passivated Si nanoparticles and clarify the physical origin of its strong photoluminescence, we have performed the valence-band photoemission measurements with photon energy of 184.1 eV as shown in Fig. 1. In Fig. 1, the spectral features around 3.5, 9, and 11 eV in binding energy originate from the Si 3*p*- and 3*s*-derived states, and those around 5.5 and 7 eV in binding energy originate from the C 2*p*-derived states in Si-C σ bonds and butyl passivants. Other features originate from the uncovered region of HOPG substrate. In the inset of Fig. 1, we plot the photoemission spectrum in the vicinity of Fermi level. As shown in the inset of Fig. 1, we have taken into account the contributions from Si nanoparticles and the uncovered region of semimetallic HOPG substrate and have estimated the valence-band maximum of about 2 eV below the Fermi level. Therefore, the energy gap of the present butyl-passivated Si nanoparticles is considered to be about 4 eV, which is modified by the quantum confinement effect. This value corresponds to the absorption edge in extinction spectrum and resonance in PLE spectrum, and therefore, the present photoluminescence is considered to originate from the electron-hole pair recombination between the modified valence-band and conduction-band due to the quantum size effect.

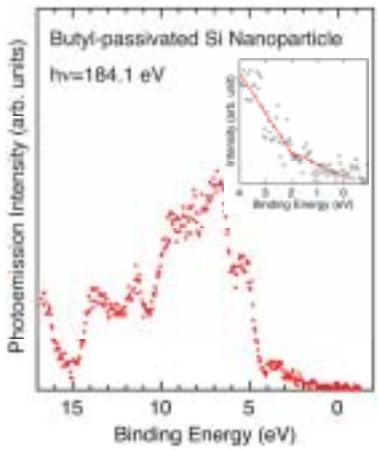

Fig. 1 Valence-band photoemission spectrum of butyl-passivated Si nanoparticle with mean diameter less than 3 nm on the HOPG substrate at room temperature measured with $h\nu$=184.1 eV. The inset shows the photoemission spectrum in the vicinity of Fermi level.

[1] *For example*, L. T. Canham, Appl. Phys. Lett **57** (1990) 1046.

[2] R. Saito, T. Kamikake, A. Tanaka, and H, Yasuda, Trans. Mat. Res. Soc. Jpn. (2006) in press.

BL8B1

Characterization of Lithium in Metal Oxide by an XAFS Method

T. Kurisaki[1], Y. Inoue[1], H. Tsutsumi[1], H. Yamashige[1], H. Wakita[1,2]

[1]*Department of Chemistry, Faculty of Science, Fukuoka University, Nanakuma, Jonan-ku, Fukuoka 814-0180, Japan*

[2]*Advanced Materials Institute, Fukuoka University, Nanakuma, Jonan-ku, Fukuoka 814-0180, Japan*

Lithium compounds are generally used in lithium batteries, lithium glasses and other materials. However, there are a few reports about Li-K absorption spectra [1]. Therefore, it is very interesting to investigate the chemical bonding condition of lithium compounds by comparing the experimental and theoretical spectra.

In this work, we applied the X-ray absorption near edge structure (XANES) spectroscopy to lithium compounds. X-ray absorption spectra of near Li K absorption edges were (XAFS) measured at BL8B1 of the UV-SOR in the Institute of Molecular Science, Okazaki [2]. The energy of the UVSOR storage ring was 750MeV and the stored current was 110-230 mA. The absorption was monitored by the total electron yield using a photomultiplier. We employed the discrete variational (DV)-Xα molecular orbital (MO) method to perform calculated spectra, and compared observed spectra with calculated spectra.

The Li *K* XANES spectra for six lithium compounds are shown in Fig. 1. A remarkable change of the spectral patterns was observed for the lithium hardies and other lithium compounds.

The observed and calculated Li K XANES spectra for lithium chloride are shown in Fig. 2. The peaks that appear at approximately 65, 66, 67.5 and 68.5 eV on experimental spectrum are labeled A, B, C and D in the order of increasing energy, respectively. The peaks A and B are estimated to the electron transition (mainly Li 1s to unoccupied mixed orbital consisting of Li 2s, Li2p Cl 3p and Cl 4s).

[1] J. Tsuji, K. Kojima, S. Ikeda, H. Nakamatsu, T. Mukoyama and K. Taniguchi, J. Synchrotron Rad. **8** (2001) 554.

[2] S. Murata, T. Matsukawa, S. Naoe, T. Horigome, O. Matsuodo, and M. Watanabe, Rev. Sci. Instrum. **63** (1992) 1309.

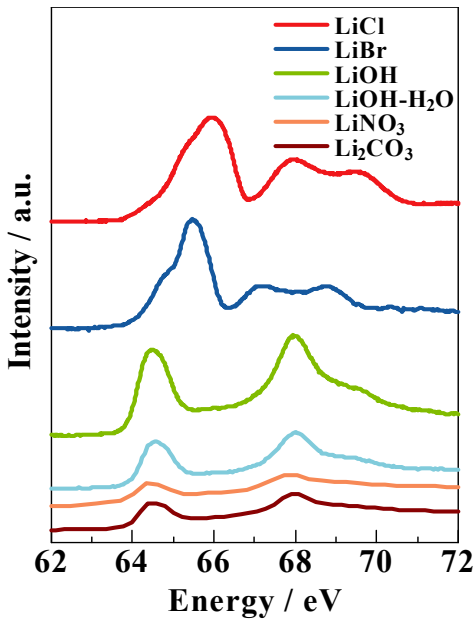

Fig. 1 Li K-edge XANES Spectra of Lithium Compounds.

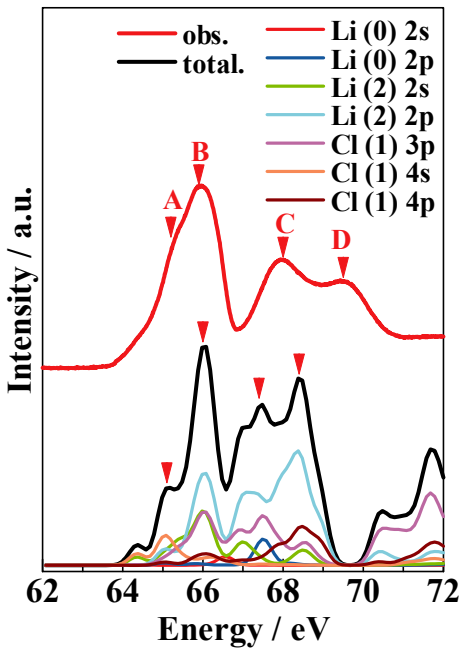

Fig. 2 Observed and Calculated Li K-edge XANES Spectra of Lithium Chloride.

BL8B1

The Study on the Local Structural Change of FIB–CVD DLC by Annealing

A. Saikubo, Y. Kato, K. Kanda, S. Matsui

Graduate School of Science, Laboratory of Advanced Science and Technology for Industry, University of Hyogo, 3–1–2 Kouto, Kamigori–cho, Ako–gun, Hyogo 678–1205, Japan

Introduction

It is known that focused ion beam–chemical vapor deposition (FIB–CVD) is useful to fabricate three dimensional nano structures. The fundamental structure of carbon thin film formed by FIB–CVD has been reported to be diamond like carbon (DLC) from the measurement of Raman spectrum and near edge x–ray absorption fine structure (NEXAFS) of K absorption edge of carbon [1,2]. It was known that the gallium using as an ion source remained in the FIB–CVD DLC. Moreover, it was recognized that the gallium located at the center of the FIB–CVD DLC moved toward the surface of DLC by annealing [3]. In the present work, we investigated the relation between the movement of gallium in the FIB–CVD DLC and the annealing at the temperature of 200°C and 600°C. The NEXAFS spectrum for K edge absorption of carbon was measured with the change of the incident angle of synchrotron radiation x-ray beam in order to obtain the information on the local structure along depth direction.

Experiment

The measurement of NEXAFS spectra for FIB–CVD DLC were performed at BL8B1 of UVSOR in Institute for Molecular Science, which was synchrotron radiation facility with 0.75 MeV electron storage ring. The beamline provides the photons with the desired energy in the energy range of 30–800 eV by using the monochromator with three gratings. The energy range of 275–320 eV, which is the energy range near K edge absorption for carbon, was extracted by using 540 lines/mm laminar grating which had a 15 m radius. The energy resolution was estimated to be approximately 0.5 eV in full width at half maximum. The reading of monochromator was calibrated by making use of the peak of the resonance transition from 1s orbital to π^* orbital observed at 285.3 eV in the spectrum of graphite. The detection of photocurrent coming from the sample was performed in the total electron yield. The intensity of incident x–ray was measured by detecting the photocurrent coming from gold film using as a sample for the measurement of incident x–ray intensity. The absorption intensity was measured by detecting the photocurrent coming from the sample. In this measurement, the NEXAFS spectra of FIB–CVD DLC were measured for the incident angle of the synchrotron radiation x-ray beam from 0° to 60° by 15° step.

Result and Discussion

The NEXAFS spectra of measured at incident angle of 60° for each annealing temperature of 200°C, 400°C and 600°C are shown in Fig. 1. The sharp peak located at 285.3 eV and the broad peak located on the high energy side of ~293 eV is assignable to the resonance transition from 1s orbital to π^* orbital originating from sp^2 sites and σ^* orbital originating from sp^2 and sp^3 sites, respectively. Moreover, in the NEXAFS spectrum of FIB–CVD DLC, the peak which is assignable to the resonance transition from 1s orbital to σ^* orbital originating from carbon bonding to gallium appears at 289.0 eV [2]. For the FIB–CVD DLC annealed at 400°C, the peak intensity observed at 289.0 eV increases remarkably. This indicates that the gallium distributed inside FIB–CVD DLC moves to the vicinity of surface. On the other hand, the peak intensity located at 285.3 eV decreases. Considering these experimental results, the gallium moved from the inside of FIB–CVD DLC to the vicinity of surface is considered to couple to the carbon atom by decoupling the carbon double bonding. For the FIB–CVD DLC annealed at 600°C, it is considered that the carbon double bonding is generated because the gallium in the FIB–CVD DLC departs from that.

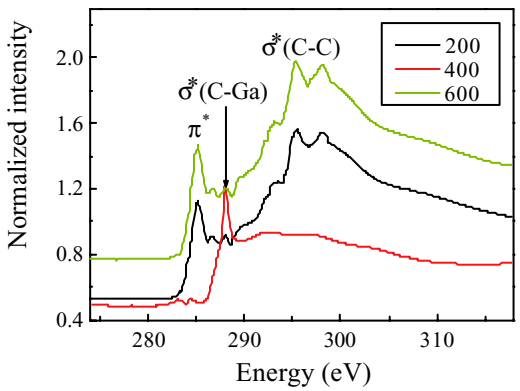

Fig. 1 NEXAFS spectra of FIB–CVD DLC measured at incident angle of 60° for each annealing temperature of 200°C, 400°C and 600°C.

[1] S. Matsui *et al.*, J. Vac. Sci. Tech. B **18** (2000) 3181.
[2] K. Kanda *et al.*, to be published in Rad. Phys. Chem.
[3] J. Fujita *et al.*, Jpn. J. Appl. Phys. **41** (2002) 4423.

BL8B2

Impacts of Intermolecular Scattering on Photoelectron Angular Distribution for Well-Ordered Phthalocyanine Doublelayer

S. Kera[1], T. Hanatani[1], H. Fukagawa[1],
S. Nagamatsu[1], R. Sumii[2], H. Yamane[2], K.K. Okudaira[1], N. Ueno[1]
[1]*Faculty of Engineering, Chiba University, Chiba 263-8522 Japan*
[2]*Graduate School of Science, Nagoya University, Nagoya University, Nagoya 464-8602 Japan*

Angle-resolved ultraviolet photoelectron spectroscopy (ARUPS) has been known as a powerful technique to obtain crucial information on an electronic band structure for various kinds of materials. Moreover, for organic thin films, information on the geometrical structure of the thin films can be also discussed in accordance with a qualitative analysis according to the selection rule with polarization dependence. However, it is believed that the quantitative analysis of the ARUPS intensity to obtain structural information is difficult due to a lack of a standard/simple theoretical model.

The observed take-off angle (θ) dependences of HOMO bands in ARUPS spectra of well-ordered OTi- (or OV-) phthalocyanine (Pc) monolayer and doublelayer were compared with calculated results to clarify the intermolecular effects on the angular distribution.

Experiments

ARUPS spectra were measured at photon incidence angle $\alpha=70^{o}$, hν=20-40 eV, and T=295 K. θ dependence of ARUPS spectra was analyzed using the single-scattering approximation combined with molecular orbital calculation (SS/MO) [1]. The purified Pc molecules were carefully evaporated onto the HOPG. Characterization of the monolayer and doublelayer formation as well as the molecular orientation has been carried out for Pc/graphite systems [2,3]. Coverage of the film can be estimated from the work function as discussed in the previous paper [3].

Results and Discussion

Figure 1(a) shows θ dependence of ARUPS of annealed-OTiPc doublelayer on HOPG. The intensity is normalized to the incidence photon flux and the background is subtracted. The HOMO band is assigned to a single π MO as in CuPc [4] (inset of Fig.1). For the doublelayer, HOMO band is observed as two prominent peaks (labeled A and B). Peak A is related to photoemission from the underlying 1st layer, in which molecules are oriented flat with O-atom protruding vacuum side. Peak B is assigned as photoemission from the 2nd layer, where molecules are oriented reversely. Figure 1(b) shows the comparison between observed and calculated θ dependences of the HOMO-band intensities. In this fitting, the observed θ pattern of the peak B is well reproduced by the SS/MO calculation. However, peak A shows marked disagreement with the SS/MO. The disagreement suggests there is a strong scattering effect of photoelectron from the underlying layer, since for the oriented monolayer the HOMO-band angular distribution is well reproduced by the calculation as for peak B in Fig.1(b). Now we are trying to get a calculated pattern of peak A by taking into account the intermolecular effects between 1st and 2nd layer in various molecular arrangement and orientations.

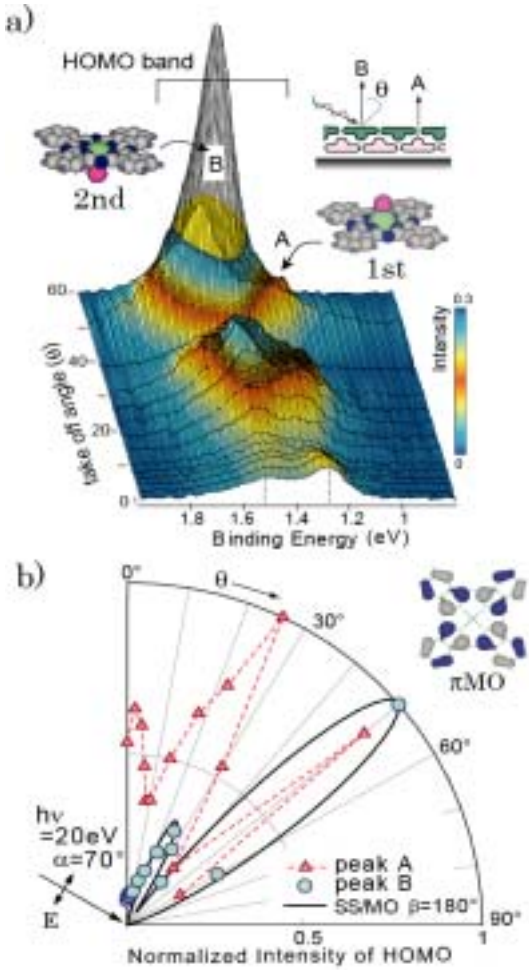

Fig. 1 (a) θ dependence of ARUPS of 2-ML-OTiPc on HOPG. (b) Comparison with the observed and calculated θ patterns of the HOMO-band A and B. β is tilt angle of a molecular plane.

[1] N. Ueno *et al*., J. Chem. Phys. **107** (1997) 2079.
[2] H. Yamane *et al*., J. Elec. Spec. Relat. Phenom. **137-140** (2004) 223.
[3] H. Fukagawa *et al*., Phys. Rev. B **73** (2006) 14302(R).
[4] S. Kera *et al*., Chem. Phys. Lett. **364** (2002) 93.

BL8B2

Electronic Structure of $LiNi_{1-x}M_xO_2$ Mixed Oxides (II)

T. Miyazaki[1], Y. Komatsu[1], D. Yoshimura[2], R. Sumii[2], T. Yamaguchi[1]

[1]*Department of Applied Chemistry, Faculty of Engneering, Ehime University, Matsuyama 790-8577 Japan*

[2]*Research Center for Materials Science, Nagoya University, Nagoya 464-8602, Japan*

Lithium and nickel mixed oxide ($LiNiO_2$) has a two-dimensional triangular lattice in lamellar structure in which lithium and nickel are alternately and regularly arranged to oxygen layers. The surface lattice oxygen progresses as a reduction/oxidation (redox) catalyst for the oxidative coupling of methane (OCM). The top valence band structures usually determine the electronic properties and surface catalysis of the materials. Therefore, it should be carefully investigated that the electronic structure led to intense experimental approach to the Ni3d and O2p states. Ultraviolet photoelectron spectroscopy (UPS) was surface sensitive technique and effective for the top valence band structures which determined the activities of the selective oxidation. In this study the comparison of $LiNiO_2$ and $LiNi_{1-x}M_xO_2$ (M = Mn, Ti, Al, Fe, Co, Te; $0 \leq x < 0.2$) which replaced the part of Ni with other transition metal element. Also, Ar^+ bombardment was done in order to imitate dynamic redox surface and remove the contamination such as carbonates.

$LiNi_{1-x}M_xO_2$ (M = Mn, Ti, Al, Fe, Co, Te; $0 \leq x < 0.2$) were prepared from $LiNO_3$, $Ni(OH)_2$ and $M(NO_3)_n$ by the solid-state reaction. UPS spectra were measured for the incident photon energy ($h\upsilon$=30~75eV) using photoelectron spectroscopy equipment (BL8B2) of UVSOR facility in IMS. The Fermi energy of the UPS system was determined by using the Fermi edge of gold films. The total resolution was found to be about 0.3eV in the photon energy region of $30 \leq h\upsilon \leq 75$eV by measuring the Fermi edge of gold. A sample surface processing by Ar^+ bombardment or heating of infrared radiation was carried out as a pretreatment.

Figure 1 exemplified the UPS spectra of $LiNiO_2$, $LiNi_{0.9}Mn_{0.1}O_2$ and $LiNi_{0.9}Ti_{0.1}O_2$ with reference to E_F as the zero of the energy scale and the Gaussian curve fitted data. The overall features in the spectra of NiO were similar as far as the peak positions were concerned. There were at least five structures on the top valence region. These curve made up from five individual bands consistently matched with the observed spectra. The peak position of $LiNiO_2$, denoted by the characters A-E, appears in the binding energy which left at E_b = 1.6eV, 2.8eV, 5.1eV, 7.0eV and 9.8eV from the Fermi level, respectively. The band structures at E_b = 1.6 and 2.8eV should be contribution from these t_{2g} and e_g states, respectively. The bands of C and D at E_b = 5.1 and 7.0 eV should be contributed to O2p bands. The C-band of $LiNi_{0.9}Mn_{0.1}O_2$ occupied about 80% for area intensity of total O2p bands, and it was almost equivalent to 79% in case of $LiNiO_2$. The C-band area intensity of of $LiNi_{0.9}Ti_{0.1}O_2$ meanwhile increased to 87%. The C_2-selectivity was $LiNi_{0.9}Mn_{0.1}O_2$ (61%) ≤ $LiNiO_2$ (63%) < $LiNi_{0.9}Ti_{0.1}O_2$ (70%), and it was possible to conclude a direct relation in electronic structures of the metal oxide surface and the selective oxidation.

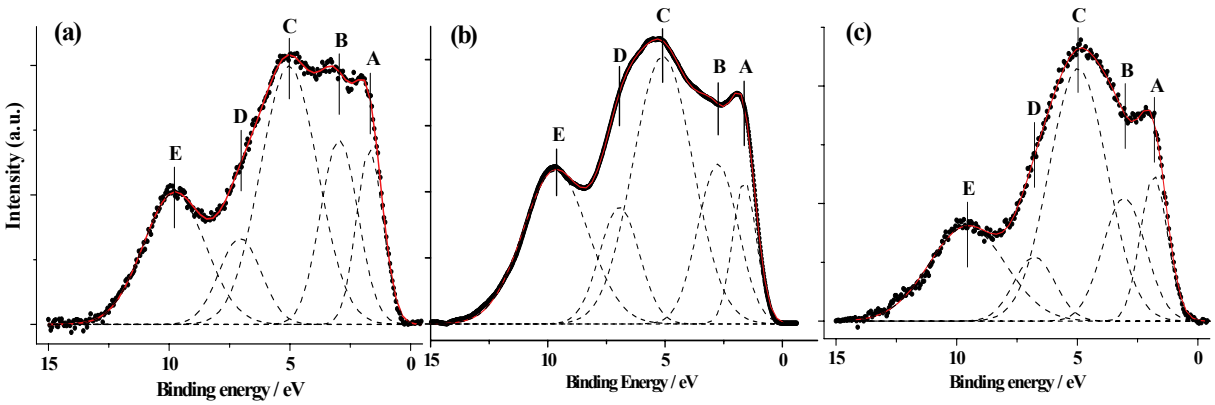

Fig.1. UPS spectra and the Gaussian fitted curves of a) $LiNi_{0.9}Mn_{0.1}O_2$, b) $LiNiO_2$ and c) $LiNi_{0.9}Ti_{0.1}O_2$.

BL8B2

Photoemission Spectroscopy Study of Bathocuproine Insertion Effect to Au/Zn-phthalocyanine Interface

S. Tanaka[1,2], Y. Yoshida[3], M. Nonomura[3], K. Yoshino[2], I. Hiromitsu[3]

[1] *Center of Integrated Research in Science, Shimane University, Matsue 690-8504 Japan*

[2] *Research Project Promotion Institute, Shimane University, Matsue 690-8504 Japan*

[3] *Faculty of Science and Engineering, Shimane University, Matsue 690-8504 Japan*

An insertion of a thin layer in the organic -material/metal-electrode interfaces is a well known technique to improve the performance of organic semiconductor devices. [1,2] We have recently observed that the hole transport from Au to Zn-phthalocyanine (ZnPc) is enhanced substantially under the forward bias condition by an insertion of a thin bathocpuroine (BCP) layer to the Au/ZnPc interface. [3] In this study, we measured the electronic energy level structures of Au/ZnPc and Au/BCP interfaces by photoemission spectroscopy in order to understand the insertion effect of a thin BCP layer.

Experimental

ZnPc and BCP were purchased from Aldrich, and were purified by vacuum sublimation. All the photoemission measurements were carried out in ultrahigh-vacuum at room temperature. The base pressure of the main chamber and the preparation chamber were about 2×10^{-8} Pa and about 2×10^{-7} Pa, respectively. Evaporation of organic molecules was performed using a glass-cell evaporator after careful outgassing, keeping the pressure of the preparation chamber at less than 4×10^{-6} Pa. The substrates were Si (100) wafers precoated with Au *in situ*. The deposition rates of the organic molecules were monitored with a quartz microbalance, using the bulk densities of 1.55 g/cm^3 for ZnPc, 1.3 g/cm^3 for BCP.

Results and Discussion

Figure 1 shows photoemission spectra of ZnPc (5nm) on Au and BCP (5nm) on Au around the Fermi level. The photoemission spectrum of Au was also shown for comparison. The thickness of 5nm was chosen for making the same structural condition using in ref. 3.

In the ZnPc spectrum, the signal from Au substrate still appeared. The 5nm thickness of ZnPc was not enough for a complete covering of the Au substrate or Au atoms were diffused from the substrate to the ZnPc layer. On the other hand, in the BCP spectrum, no signal of Au was shown. The Au substrate was completely covered by the 5nm BCP layer. This result suggests that the interaction between Au and ZnPc is more active than that between Au and BCP.

The edge energy of the highest occupied molecular orbital of ZnPc and BCP was observed at about 1.0 eV and 3.0 eV respectively from the Fermi edge of Au. This result suggests that the barrier height of the hole injection from Au to BCP is larger than that from Au to ZnPc. These result seem to be inconsistent with the increase of the dark current density, J_{dark}, from Au by the insertion of BCP layer: the J_{dark} of the Au/BCP/ZnPc/In/Al cell was larger than that of the Au/ZnPc/In/Al cell.[3] If the barrier height of the hole injection at the Au/ZnPc interface is the only factor that determines the J_{dark} of the systems (the majority carrier is the hole in this case because of the ZnPc property), the Au/BCP/ZnPc/In/Al cell should show lower J_{dark} than the Au/ZnPc/In/Al cell.

These facts can probably be explained as follows: the effect of insertion of the BCP layer is not to lower the barrier height for the hole injection at Au/ZnPc interface but to prevent an interaction between Au and ZnPc. The interaction of Au and ZnPc may increase the concentration of trapped states at the interface region of the Au/ZnPc and decrease the conductivity.

The present study suggests that the control of the interaction between an organic material and an electrode, as well as the injection barrier height from the electrode to the organic materials, is important for the control of the operation of the organic semiconductor devices.

[1] L. S. Hung, C. W. Tang, M. G. Mason, Appl. Phys. Lett., **70** (1997) 1233.

[2] F. Li, H. Tang, J. Andregg, J. Shinar, Appl. Phys. Lett., **73** (1998) 2763.

[3] M. Nonomura, I. Hirmoitsu, S. Tanaka, Appl. Phys. Lett., **88** (2006) 042111.

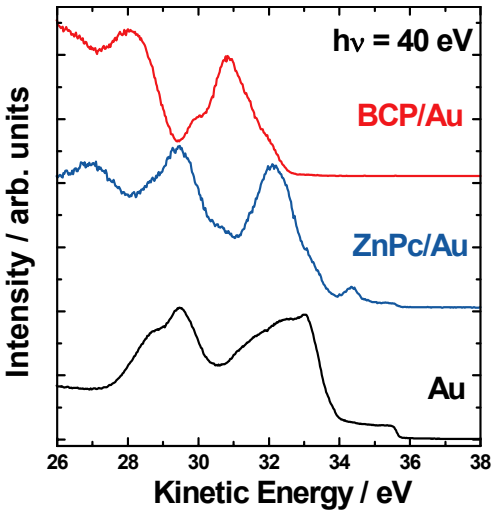

Fig. 1 Photoemission spectra of Au, ZnPc (5nm) on Au and BCP (5nm) on Au around the Fermi level.

BL8B2

Energy-Band Dispersion in Highly Ordered Thin Films of Pentacene Prepared on Cu(110)

H. Yamane [1], D. Yoshimura [2], R. Sumii [3], K. Kanai [1], Y. Ouchi [1], K. Seki [1,3]

[1] *Department of Chemistry, Nagoya University, Nagoya 464-8602, Japan*

[2] *SAGA light source, Kyushu Synchrotron Light Research Center, Saga 841-0005, Japan*

[3] *Research Center for Materials Science, Nagoya University, Nagoya 464-8602, Japan*

Introduction

Pentacene, a high hole mobility material, is one of the important organic semiconductors in realizing efficient organic devices, in particular organic field-effect transistors. Therefore, the film growth, the film structure, and the electronic structure of pentacene thin films have been studied by many research groups. Recent experimental data reflecting the progress in experimental techniques such as high energy resolution and the preparation of high quality samples point towards the necessity of using polaronic concepts to rationalize the electrical properties of organic-semiconductor films. The charge-vibration coupling and the energy-band dispersion of the highest occupied molecular orbital (HOMO) plays crucial roles in the hopping- and band-like hole transport in organic solids, respectively. In this work, in order to study the hole transport mechanism in pentacene thin films, angle-resolved ultraviolet photoemission spectroscopy (ARUPS) experiments were performed for highly ordered thin films of pentacene prepared on Cu(110).

Experiments

The take-off angle (θ) dependence of ARUPS spectra were measured at the photon energy ($h\nu$) of 20 and 30 eV, the photon incidence angle (α) of 60°, and the specimen temperature of 300 K.

The purified pentacene was carefully evaporated onto a clean Cu(110) surface heated at about 450 K. This enabled the preparation of the highly ordered monolayer.[1]

Results and Discussion

According to ref.[1], pentacene molecules deposited on Cu(110) in the monolayer regime form a highly ordered structure with a planar adsorption geometry, where the molecular long axis is parallel to the [1-10] substrate direction. We confirmed these by measuring the ARUPS spectra as a function of the azimuthal angle, using symmetry selection rule (not shown). For thick multilayers, subsequent growth proceeds with an upright molecular orientation and leads to the formation of crystalline films which are epitaxially oriented with respect to the substrate. [1]

Figure 1 shows the θ dependence of the ARUPS spectra of the pentacene monolayer on Cu(110), where the substrate electronic states are colored by yellow. The binding-energy (E_B) position is measured from the Fermi level of the substrate (E_F^{sub}) and the intensity is normalized to the incident photon flux. The feature near E_F^{sub} colored by blue can be ascribed to the charge-transfer (CT) state due to the molecule-substrate chemical interaction, which induces the large vacuum-level shift of about -1.0 eV (not shown). The HOMO appears at E_B of 0.9 eV at θ = 43°. With increasing θ, the HOMO shifts to the high-E_B side, and turns back at θ = 45°. Also, at θ = 50° and 58°, similar turn back of the peak is seen. The total shift of the HOMO is about 0.25 eV. Such a cyclic shift can also be seen for the HOMO-1. We can attribute these shifts to the energy-band dispersion of the pentacene monolayer along the [1-10] substrate direction. Analyses using the tight-binding model gave a lattice constant of about 1.6 nm, which agrees well with the lateral lattice constant of the pentacene monolayer formed on Cu(110) [1], with the estimated transfer integral of 63 meV for the HOMO band and the effective mass of the HOMO hole of 0.24 m_0.

By using the density-functional-theory method, the transfer integral for the σ-σ interaction in the pristine pentacene monolayer is calculated to be a few meV, which is much smaller than that of the experimental value of 63 meV. The observed energy-band dispersion may originate from the intermolecular interaction via the substrate due to the hybridization of the molecular orbital and the substrate.

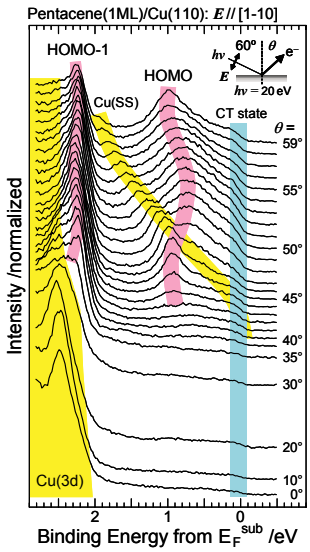

Fig. 1 ARUPS spectra of the pentacene monolayer on Cu(110). The inset shows the measurement geometry.

[1] S. Söhnchen *et al.*, J. Chem. Phys. **121** (2004) 525.